Stabilisation and characterisation of a trinuclear uranyl complex by ligand-radical formation

Mukesh K Singh,*[a] Stephen Sproules[b] and Jason B Love*[a]

Experimental Details

The synthesis of all air- and moisture-sensitive compounds was conducted using standard Schlenk techniques under an atmosphere of dry argon or within MBraun gloveboxes under an atmosphere of dry dinitrogen. Vacuum atmospheres and MBraun gloveboxes were employed for the storage and handling of air- and moisture-sensitive compounds. All glasswares were dried in a 220°C oven overnight prior to utilisation. Dry solvents were obtained from a solvent purification system (Innovation Technologies) and were stored in Teflon-tapped ampules over pre-dried 4 Å molecular sieves. $[UO_2Cl_2(THF)_3]$ and 2,4,6-tris(2-pyrimidyl)-1,3,5-triazine (TPymT) were synthesised according to reported literature.[1] 18-Crown-6 was sublimed before use. All other chemicals were utilised as received without further purification unless otherwise specified.

Single-crystal X-ray diffraction data were collected on a Supernova, Dual, Cu at zero Atlas diffractometer utilising Cu Kα radiation (λ = 1.5418 Å) at a temperature of 120 K. Structures were solved using ShelXT direct methods and were refined with a full-matrix least-squares refinement on |F|2 using ShelXL.[2] All programs were operated within the Olex2 suite.[3] Non-hydrogen atoms were refined with anisotropic displacement parameters, while hydrogen atoms were constrained to their respective parent atoms and refined using a riding model. During the refinement process, 2.25 THF solvent molecules were masked. Structures were analysed and illustrated using Mercury 4.3.1.[4]

Crystal data and structure refinement for **1.**	
Empirical formula	$C_{44}H_{67}Cl_6KN_9O_{16.25}U_3$
Formula weight	1947.95
Temperature/K	120.00(10)
Crystal system	triclinic
Space group	P-1
a/Å	13.9789(3)
b/Å	14.6991(4)
c/Å	17.4435(5)
α/°	74.253(2)
β/°	87.805(2)
γ/°	69.205(2)
Volume/Å^3	3218.28(15)
Z	2
ρ_{calc}g/cm^3	2.010
μ/mm^{-1}	7.909
F(000)	1842.0
Crystal size/mm^3	0.18 × 0.07 × 0.06
Radiation	Mo Kα (λ = 0.71073)
2Θ range for data collection/°	6.508 to 58.23
Index ranges	-19 ≤ h ≤ 18, -18 ≤ k ≤ 19, -23 ≤ l ≤ 23
Reflections collected	70525
Independent reflections	15702 [R_{int} = 0.0578, R_{sigma} = 0.0561]
Data/restraints/parameters	15702/0/613
Goodness-of-fit on F^2	0.991
Final R indexes [I>=2σ (I)]	R_1 = 0.0365, wR_2 = 0.0711
Final R indexes [all data]	R_1 = 0.0527, wR_2 = 0.0763
Largest diff. peak/hole / e Å^{-3}	2.16/-0.90

UV-vis-NIR spectroscopy was performed utilising a quartz cuvette with a path length of 10 mm on a NanoDrop 2000c photospectrometer scanning between 1100 and 300 nm under inert conditions.

A THF solution of **1** was analysed against a solvent blank over the scanning range of 400 – 4000 cm^{-1} on a Perkin Elmer Spectrum 65 FT-IR spectrometer.

Raman analysis of solid samples was conducted on a ThermoFisher Scientific DXR3 Raman microscope, employing a 785 nm excitation laser at 2 mW laser power, with an exposure time of 60 seconds and three scans. A 10x objective with a numerical aperture of 0.3 was utilised for measurements.

EPR spectra were recorded on a Bruker ELEXSYS E500 spectrometer. Spectral simulations were performed using Bruker's Xsophe software package.[5]

Synthesis

1: One equivalent of TPymT with one equivalent of potassium graphite, one equivalent of 18-Crown-6 and three equivalents of $\{UO_2Cl_2(THF)_3\}$ were stirred overnight. Following the stirring, filtration was performed, and the filtrate was concentrated and kept at -20°C for two days. As a result, dark blue needle-shaped crystals of complex **1** were formed.
Elemental analysis {[K(18-c-6)][$(UO_2Cl_2)_3$(TPymT)] 1.25 THF; $C_{32}H_{43}Cl_6KN_9O_{13.25}U_3$; Requires: C, 22.25; H, 2.51; N, 7.30; %.}
Data 1: {Found: C, 25.42; H, 4.25; N, 0.69}
Data 2: {Found: C, 19.36; H, 2.71; N, 2.12}
Data 3: {Found: C, 22.61; H, 2.22; N, 6.06}

Note: Data 1 and 3 were analysed at London Metropolitan University, London. Data 2 was collected at the Elemental Lab in London.

Computational Details

To better understand the electronic structure, Quantum Theory of Atoms in Molecules (QTAIM)[6] and Wiberg bond index analysis[7] were performed on the core structure of **1**, $[(UO_2Cl_2)_3(TPymT)]^{\bullet-}$, utilising Density Functional Theory (DFT) calculations conducted in the Gaussian16 suite of programs.[8] The $[K(18\text{-Crown-}6)]^+$ group was removed from the model complex to minimise computational costs. The hybrid B3LYP functional[9] was employed alongside a double-zeta quality basis set that utilised a CRENBL effective core potential on the U atom (which has 78 core electrons and 14 valence electrons),[10] along with a def2-TZVP basis set for O, N, Cl, and a def2-SVP basis set for the remaining atoms (C and H).[11] The broken symmetry approach was applied.[12] Infrared (IR) and Raman spectra were reproduced using the same methodology.

To replicate the experimental UV-Vis electronic transitions, time-dependent DFT (TDDFT) calculations were conducted on the core structure of **1**, $[(UO_2Cl_2)_3(TPymT)]^{\bullet-}$, using the B3LYP functional in ORCA5.0.4.[13] Cl, O, N, C, and H atoms were described by DKH-def2-TZVP basis sets, which are def2-TZVP basis sets contracted for the Douglas-Kroll Hamiltonian (DKH) as described by D. A. Pantazis. The U atoms were described by segmented all-electron relativistically contracted (SARC) basis sets of the SARC-DKH-TZVPP type.[14] The ORCA input file is provided below.

```
! B3LYP DKH DKH-def2-TZVP AUTOAUX RIJCOSX veryslowconv notrah LARGEPRINT

%tddft
nroots 100
maxdim 20
end
%scf
maxiter 1500
DIISMaxEq 40
directresetfreq 1
DampFac 0.98
DampErr 0.05
end

%basis
newgto U "SARC-DKH-TZVPP" end
newauxgto U "autoaux" end
end

* xyz 0 2
*
```

XYZ coordinates used in calculations for **1**, $[UO_2Cl_2(THF)_3]$ and $[UO_2Cl_2$(terpyridine)]

1				$\{UO_2Cl_2(THF)_3\}$				$\{UO_2Cl_2$(terpyridine)$\}$			
U	2.1780	3.2578	0.0915	U	0.1991	0.0004	-0.1323	U	-0.9192	-0.0849	0.0000
U	-3.9516	0.1979	0.0242	Cl	0.9401	-2.5867	-0.3205	Cl	-2.8239	-0.6404	1.7922
U	1.7989	-3.4646	0.1423	Cl	1.1166	2.5174	-0.3328	O	-0.5021	-1.8078	0.0000
Cl	4.7311	4.0162	0.0497	O	0.2206	-0.0013	1.6340	O	-1.2367	1.6770	0.0000
Cl	1.6870	5.6997	0.9613	O	0.0613	0.0121	-1.8921	N	0.2791	0.3980	-2.2574
Cl	-5.8472	2.0256	0.3131	O	-1.8657	-1.3396	0.0317	N	1.6757	-0.0156	0.0000
Cl	-5.9938	-1.4892	0.0536	O	2.6218	-0.0985	0.1707	C	-0.4021	0.8990	-3.3078
Cl	1.2754	-6.0442	0.5365	O	-1.8170	1.4101	0.0037	H	-1.3106	1.0720	-3.2142
Cl	4.3106	-4.1904	0.5847	C	-2.2020	-2.1286	1.2148	C	0.2138	1.1651	-4.5257
O	2.0450	3.6118	-1.6278	H	-1.4532	-2.6904	1.4735	H	-0.2738	1.5199	-5.2337
O	2.2823	2.7569	1.7605	H	-2.4262	-1.5487	1.9594	C	1.5472	0.8941	-4.6668
O	-3.9722	0.2513	-1.7290	C	-3.3254	-2.9293	0.8444	H	1.9744	1.0604	-5.4764
O	-3.7628	0.0962	1.7612	H	-4.1365	-2.5578	1.2245	C	2.2566	0.3751	-3.6035
O	1.8470	-3.7692	-1.5915	H	-3.2154	-3.8319	1.1831	H	3.1597	0.1728	-3.6971
O	1.6426	-3.1145	1.8583	C	-3.4241	-2.9525	-0.6302	C	1.6095	0.1558	-2.3883
N	-0.4765	3.5544	-0.1428	H	-4.3412	-2.8118	-0.9124	C	2.3151	-0.2660	-1.1663
N	-2.6141	2.4876	-0.2234	H	-3.1189	-3.8048	-0.9786	C	3.5876	-0.8677	-1.2003
N	-1.3928	0.0872	0.0223	C	-2.5522	-1.8473	-1.1134	H	4.0079	-1.0533	-2.0086
N	-2.8132	-2.1671	-0.3084	H	-1.9184	-2.1773	-1.7689	C	4.1959	-1.1744	0.0000
N	-0.8003	-3.4701	-0.1578	H	-3.0876	-1.1492	-1.5242	H	5.0255	-1.5934	0.0000
N	0.6128	-1.2022	0.0354	C	3.3284	-0.3968	1.3721	Cl	-2.8239	-0.6404	-1.7922
N	3.1983	-1.3557	-0.5815	H	3.2014	-1.3277	1.6103	N	0.2791	0.3980	2.2574
N	3.3214	1.0268	-0.6289	H	2.9956	0.1531	2.0993	C	-0.4021	0.8990	3.3078
N	0.7245	1.1712	-0.0559	C	4.7386	-0.1274	1.1529	H	-1.3106	1.0720	3.2142
C	-0.6177	1.1799	-0.0063	H	5.0277	0.6140	1.7077	C	0.2138	1.1651	4.5257
C	-1.2780	2.4756	-0.1043	H	5.2661	-0.9067	1.3835	H	-0.2738	1.5199	5.2337
C	-1.0671	4.7221	-0.3950	C	4.9144	0.1924	-0.2172	C	1.5472	0.8941	4.6668
H	-0.5340	5.5075	-0.4421	H	5.5869	-0.3829	-0.6154	H	1.9744	1.0604	5.4764
C	-2.4277	4.8265	-0.5868	H	5.1981	1.1145	-0.3163	C	2.2566	0.3751	3.6035
H	-2.8333	5.6618	-0.7892	C	3.5790	-0.0216	-0.8860	H	3.1597	0.1728	3.6971
C	-3.1791	3.6809	-0.4763	H	3.3718	0.7170	-1.4795	C	1.6095	0.1558	2.3883
H	-4.1226	3.7327	-0.5827	H	3.5823	-0.8428	-1.4027	C	2.3151	-0.2660	1.1663
C	-0.7260	-1.1027	0.0420	C	-2.5984	1.5729	1.1909	C	3.5876	-0.8677	1.2003
C	-1.4904	-2.3136	-0.1171	H	-2.0233	1.5874	1.9726	H	4.0079	-1.0533	2.0086
C	-3.4815	-3.2936	-0.6462	H	-3.2265	0.8395	1.2834				
H	-4.4143	-3.2428	-0.8158	C	-3.3232	2.8604	1.0615				
C	-2.8556	-4.4977	-0.7502	H	-4.2730	2.7074	0.9381				
H	-3.3346	-5.2748	-1.0124	H	-3.1960	3.4063	1.8527				
C	-1.5128	-4.5598	-0.4638	C	-2.7425	3.5242	-0.1288				
H	-1.0765	-5.4035	-0.4857	H	-3.4208	4.0250	-0.6091				
C	1.2906	-0.0507	-0.0747	H	-2.0296	4.1295	0.1287				
C	2.6966	-0.1305	-0.3989	C	-2.2294	2.4464	-0.9442				
C	4.4140	-1.4308	-1.1365	H	-1.4746	2.7471	-1.4740				
H	4.8082	-2.2799	-1.2956	H	-2.9170	2.1113	-1.5408				
C	5.0952	-0.2867	-1.4791								
H	5.9361	-0.3399	-1.9168								
C	4.5480	0.9235	-1.1846								
H	5.0401	1.7140	-1.3721								

Table S1. Selected bond distances and angles for **1**.

Atom	Atom	Length/Å
U1	Cl1	2.6638(12)
U1	Cl2	2.6383(12)
U1	O1	1.760(3)
U1	O2	1.746(3)
U1	N1	2.681(4)
U1	N8	2.608(4)
U1	N9	2.547(4)
U2	Cl3	2.6489(13)
U2	Cl4	2.6492(14)
U2	O3	1.754(3)
U2	O4	1.751(3)
U2	N2	2.663(4)
U2	N3	2.562(4)
U2	N4	2.646(4)
U3	Cl5	2.6614(13)
U3	Cl6	2.6516(13)
U3	O5	1.761(3)
U3	O6	1.758(3)
U3	N5	2.616(4)
U3	N6	2.556(4)
U3	N7	2.633(4)
U3	K1[1]	4.4964(12)
Cl5	K1[1]	3.3412(18)
Cl6	K1[1]	3.1686(18)
K1	O7	2.800(4)
K1	O8	2.872(4)
K1	O9	2.795(4)
K1	O10	2.900(4)
K1	O11	2.769(4)
K1	O12	2.901(4)

Atom	Atom	Atom	Angle/˚
O2	U1	O1	174.85(15)
Cl2	U1	Cl1	85.41(4)
O4	U2	O3	174.28(17)
Cl3	U2	Cl4	83.49(4)
O6	U3	O5	176.15(16)
Cl6	U3	Cl5	84.05(4)
U3	Cl5	K1	96.36(4)
U3	Cl6	K1	100.79(4)

a-axis

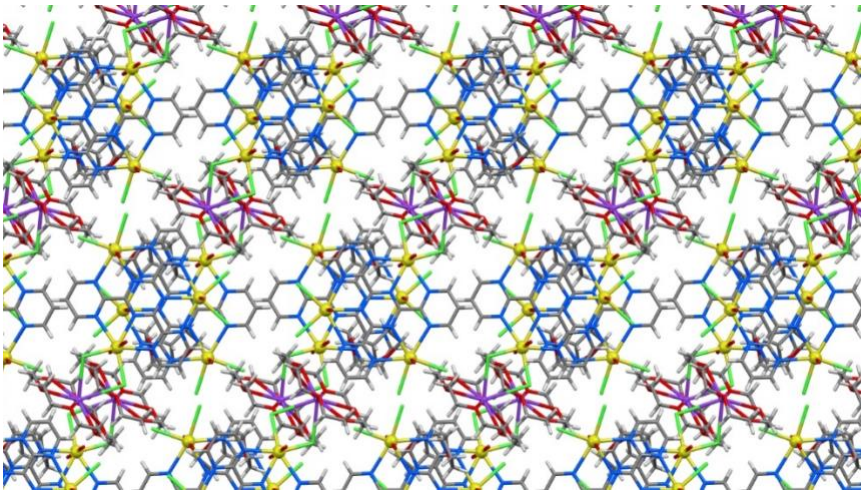

b-axis

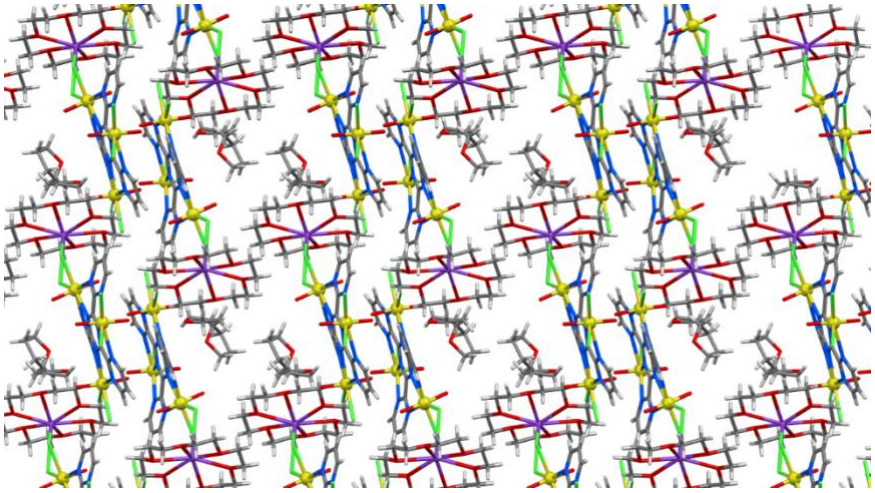

c-axis

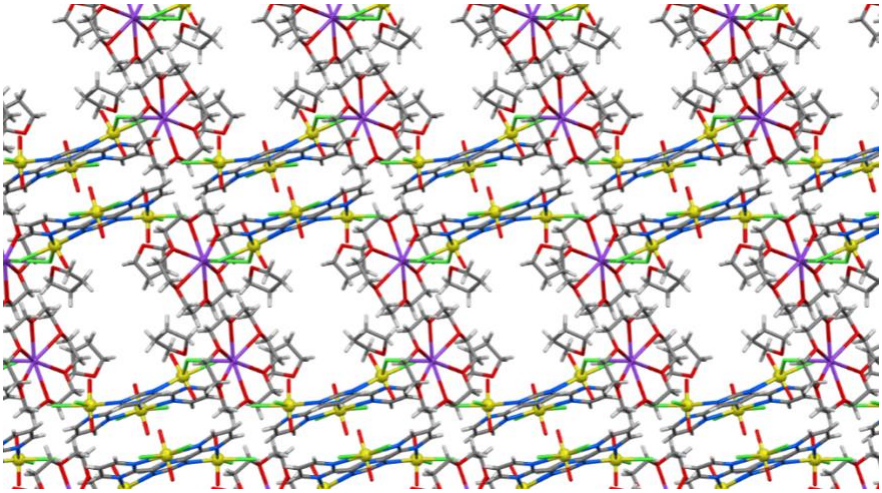

Fig. S1: The packing in the X-ray structure of **1** displayed along the a-axis (TOP), b-axis (MIDDLE) and c-axis (BOTTOM). Both a and b-axis show intermolecular π(TPymT)··· π(TPymT) and U=O···π(TPymT) interactions, whereas the c-axis shows intermolecular U-Cl···H(TPymT) interaction.

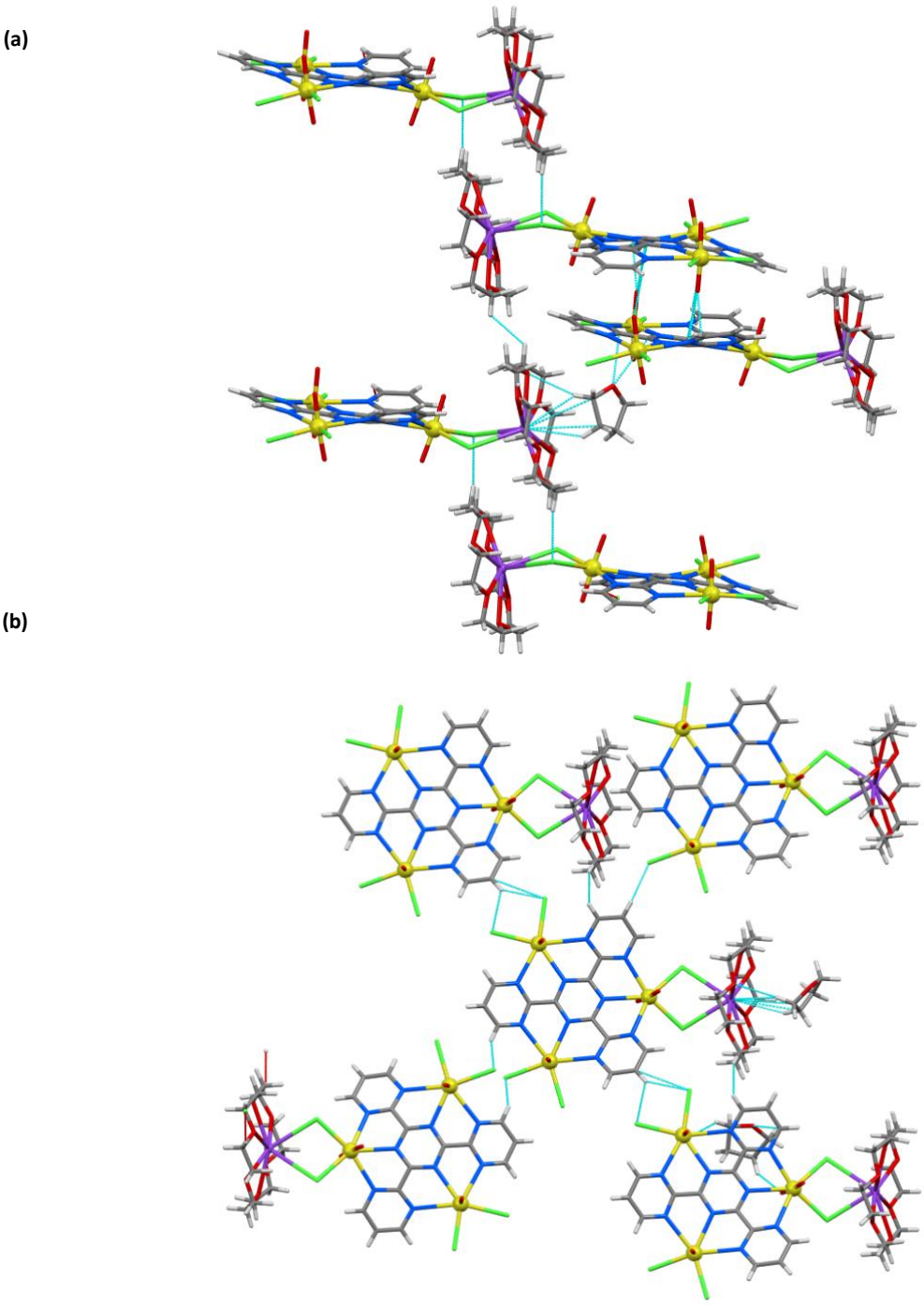

Fig. S2: The short contacts shown from the (a) side and (b) top view with respect to the $[(UO_2Cl_2)_3(TPymT)]$ molecular plane.

Table. S2: DFT computed QTAIM parameters for U-O_{yl}, U-Cl, U-N(TPymT), U-N(TerPy) and U-O(THF) bond critical points (BCPs) for **1**, [$UO_2Cl_2(THF)_3$] and related [UO_2Cl_2(terpyridine)] complexes. Greater total electron density (ρ), along with negative Laplacian of electron density ($\nabla^2\rho$) and energy density (H(r)) at the U-Oyl bond critical point (BCP), suggests stronger polar covalent bonding for a given bond.

			Eigen value of Hessian						
1	BCP no.	Electron density ρ (e Bohr^{-3})	λ_1	λ_2	λ_3	Laplacian of electron density ($\nabla^2\rho$) e Bohr^{-5}	*Energy density H(r)* e Bohr^{-3}	Ellipticity (ε)	Bond dist. (Å)
U1O1	224	0.3160	-0.5962	-0.5921	1.6303	0.4420	-0.2828	0.0070	1.760
U1O2	213	0.3275	-0.6299	-0.6204	1.6875	0.4373	-0.3019	0.0153	1.746
U2O3	104	0.3205	-0.6094	-0.6033	1.6558	0.4431	-0.2904	0.0102	1.754
U2O4	101	0.3241	-0.6212	-0.6106	1.6686	0.4368	-0.2962	0.0173	1.750
U3O5	168	0.3153	-0.5932	-0.5922	1.6333	0.4479	-0.2816	0.0016	1.761
U3O6	155	0.3187	-0.6016	-0.5942	1.6299	0.4341	-0.2866	0.0124	1.758
U1Cl1	235	0.0627	-0.0628	-0.0590	0.2726	0.1507	-0.0116	0.0646	2.664
U1Cl2	220	0.0662	-0.0677	-0.0629	0.2868	0.1563	-0.0133	0.0771	2.638
U2Cl3	98	0.0647	-0.0658	-0.0608	0.2812	0.1545	-0.0126	0.0829	2.649
U2Cl4	94	0.0646	-0.0660	-0.0611	0.2814	0.1543	-0.0125	0.0801	2.649
U3Cl5	141	0.0623	-0.0636	-0.0594	0.2760	0.1530	-0.0112	0.0693	2.661
U3Cl6	177	0.0635	-0.0655	-0.0601	0.2813	0.1557	-0.0118	0.0899	2.652
U1N1	191	0.0394	-0.0439	-0.0388	0.2064	0.1237	-0.0012	0.1335	2.681
U1N8	219	0.0461	-0.0541	-0.0475	0.2457	0.1441	-0.0025	0.1398	2.608
U1N9	193	0.0525	-0.0638	-0.0552	0.2867	0.1677	-0.0039	0.1564	2.547
U2N2	116	0.0410	-0.0466	-0.0407	0.2157	0.1284	-0.0015	0.1443	2.663
U2N3	117	0.0511	-0.0621	-0.0537	0.2785	0.1628	-0.0035	0.1569	2.561
U2N4	102	0.0426	-0.0490	-0.0430	0.2247	0.1327	-0.0018	0.1402	2.646
U3N5	138	0.0467	-0.0551	-0.0480	0.2393	0.1361	-0.0031	0.1484	2.616
U3N6	161	0.0524	-0.0644	-0.0562	0.2802	0.1596	-0.0043	0.1445	2.557
U3N7	180	0.0451	-0.0524	-0.0461	0.2308	0.1323	-0.0028	0.1377	2.632
K-Cl5	151	0.0074	-0.0053	-0.0050	0.0408	0.0305	0.0018	0.0471	3.341
K-Cl6	181	0.0106	-0.0082	-0.0081	0.0619	0.0456	0.0024	0.0138	3.168
$UO_2Cl_2(THF)_3$									
UO1	63	0.31145	-0.59055	-0.57546	1.60616	0.44015	-0.27504	0.02646	1.766
UO2	70	0.31321	-0.58133	-0.57839	1.58961	0.42989	-0.27761	0.03222	1.765
UCl1	59	0.05903	-0.03692	0.23093	-0.05416	0.13984	-0.00987	0.09085	2.698
UCl2	81	0.06027	-0.02402	0.22256	-0.05543	0.14311	-0.01040	0.07771	2.687
UO-THF^3	61	0.05382	0.21726	0.05654	-0.06197	0.21182	-0.00291	0.04646	2.467
UO-THF^2	67	0.05588	0.35082	-0.06623	-0.06132	0.22328	-0.00318	0.04219	2.444
UO-THF^1	76	0.05328	0.20733	0.06871	-0.06098	0.21506	-0.00240	0.09016	2.464
UO_2Cl_2(terpyridine)									
U1O1	42	0.30777	-0.44522	1.45070	-0.57668	0.42880	-0.26846	0.01233	1.773
U1O2	72	0.29538	-0.47884	1.44902	-0.54229	0.42789	-0.24876	0.00605	1.790
U1Cl1	63	0.06179	0.10309	-0.04481	0.08649	0.14477	-0.01125	0.06983	2.674
U1Cl2	52	0.06179	0.10309	-0.04481	0.08649	0.14477	-0.01125	0.06983	2.674
U1N1	58	0.04805	0.01062	-0.03939	0.17113	0.14236	-0.00339	0.13968	2.601
U1N2	59	0.04719	0.25170	-0.04818	-0.05570	0.14783	-0.00285	0.14322	2.596
U1N3	67	0.04805	0.01062	-0.03939	0.17113	0.14236	-0.00339	0.13968	2.601

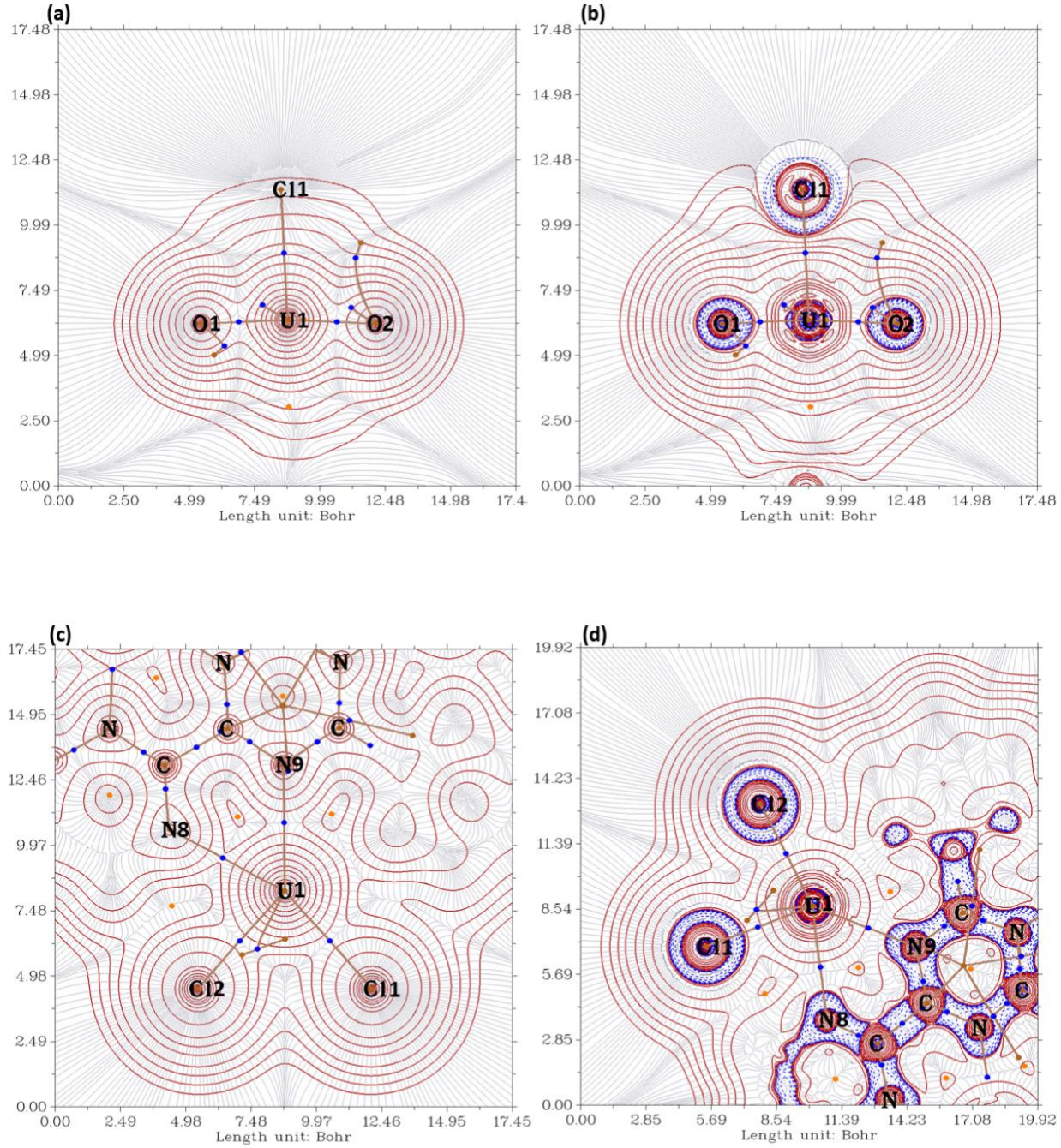
(a)
Cl1
O1
U1
O2
Length unit: Bohr
(b)
Cl1
O1
U1
O2
Length unit: Bohr
(c)
N
N
N
C
C
C
N9
N8
U1
Cl2
Cl1
Length unit: Bohr
(d)
Cl2
U1
Cl1
C
N
N9
C
C
N8
C
N
N
Length unit: Bohr

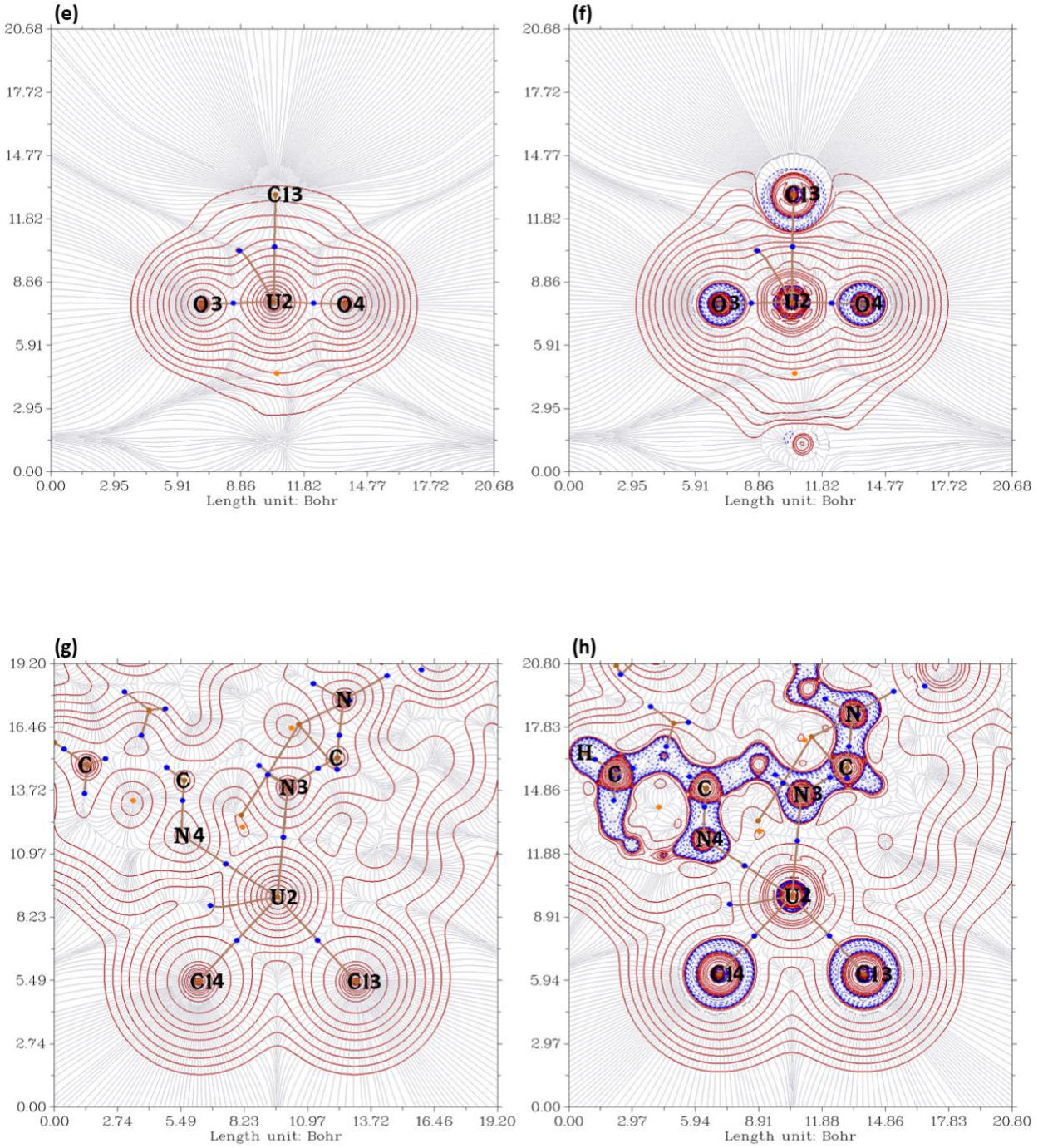
(e)
20.68
17.72
14.77
11.82
8.86
5.91
2.95
0.00
Cl3
O3
U2
O4
0.00 2.95 5.91 8.86 11.82 14.77 17.72 20.68
Length unit: Bohr
(f)
20.68
17.72
14.77
11.82
8.86
5.91
2.95
0.00
Cl3
O3
U2
O4
0.00 2.95 5.91 8.86 11.82 14.77 17.72 20.68
Length unit: Bohr
(g)
19.20
16.46
13.72
10.97
8.23
5.49
2.74
0.00
N
C
C
C
N3
N4
U2
Cl4
Cl3
0.00 2.74 5.49 8.23 10.97 13.72 16.46 19.20
Length unit: Bohr
(h)
20.80
17.83
14.86
11.88
8.91
5.94
2.97
0.00
N
H
C
C
C
N3
N4
U2
Cl4
Cl3
0.00 2.97 5.94 8.91 11.88 14.86 17.83 20.80
Length unit: Bohr

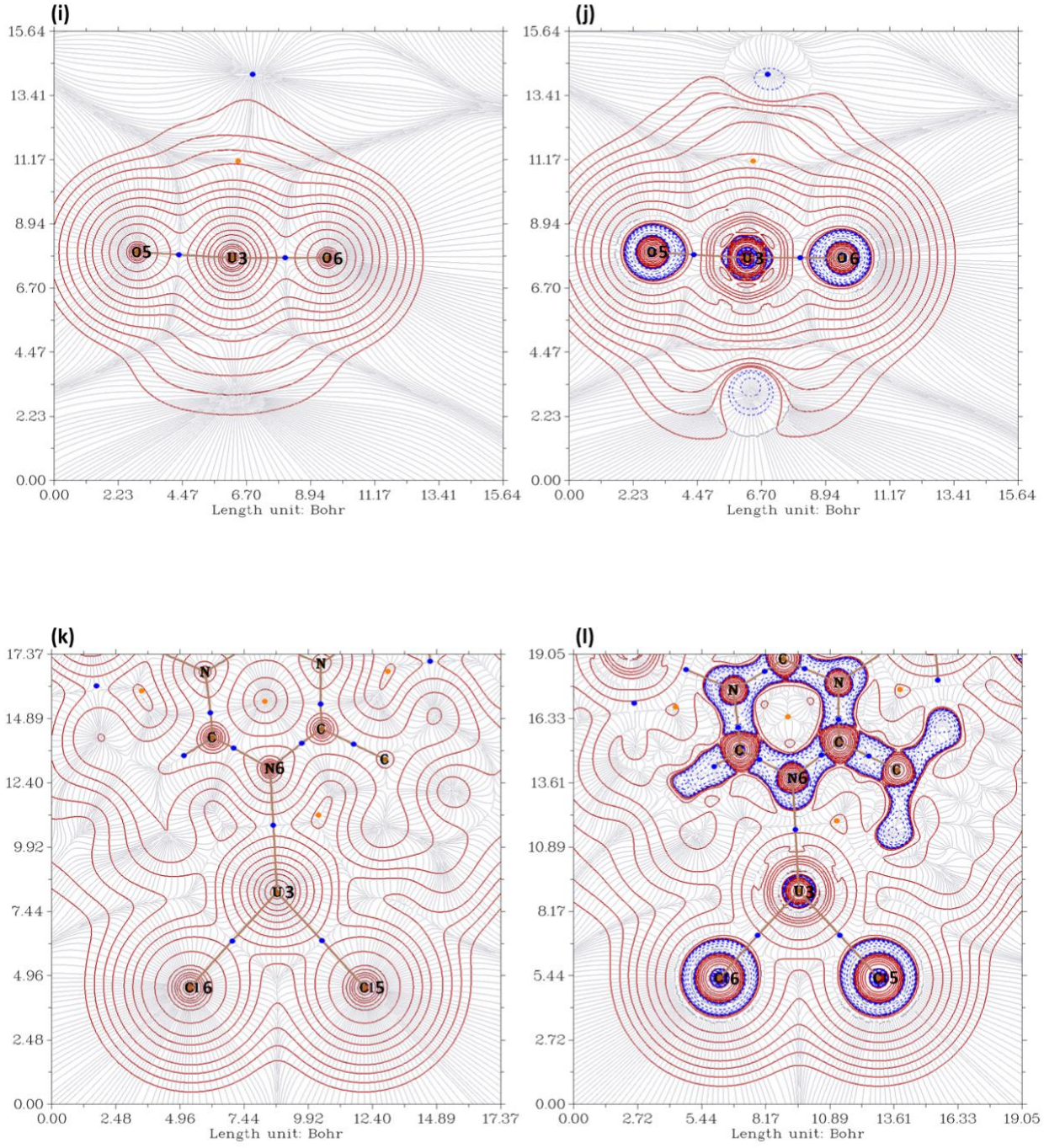

Fig. S3: DFT-QTAIM computed gradient line maps of (a,c,e,g,i,k) total electron density and (b,d,f,h,j,l) Laplacian electron density for **1**.

Table. S3: DFT computed Wiberg bond index matrix in the NAO basis for **1**, $[UO_2Cl_2(THF)_3]$ and related $[UO_2Cl_2$(terpyridine)] complexes.

1	Wiberg bond index	Bond distance (Å)
U1O1	2.1588	1.760
U1O2	2.1868	1.746
U2O3	2.1657	1.754
U2O4	2.1842	1.750
U3O5	2.1343	1.761
U3O6	2.1914	1.758
U1Cl1	1.0090	2.664
U1Cl2	1.0421	2.638
U2Cl3	1.0302	2.649
U2Cl4	1.0149	2.649
U3Cl5	0.9302	2.661
U3Cl6	0.9354	2.652
U1N1	0.3004	2.681
U1N8	0.3366	2.608
U1N9	0.3575	2.547
U2N2	0.3105	2.663
U2N3	0.3516	2.561
U2N4	0.3223	2.646
U3N5	0.3653	2.616
U3N6	0.3610	2.557
U3N7	0.3505	2.632
K-Cl5	0.0233	3.341
K-Cl6	0.0262	3.168
$UO_2Cl_2(THF)_3$		
U1O1	2.1193	1.766
U1O2	2.1439	1.765
U1Cl1	0.9290	2.698
U1Cl2	0.9468	2.687
U1O3-THF[1]	0.3284	2.467
U1O4-THF[2]	0.3532	2.444
U1O5-THF[3]	0.3328	2.464
UO_2Cl_2(TerPy)		
U1O1	2.1554	1.773
U1O2	2.1324	1.790
U1Cl1	1.0148	2.674
U1Cl2	1.0148	2.674
U1N1	0.3584	2.601
U1N2	0.3262	2.596
U1N3	0.3584	2.601

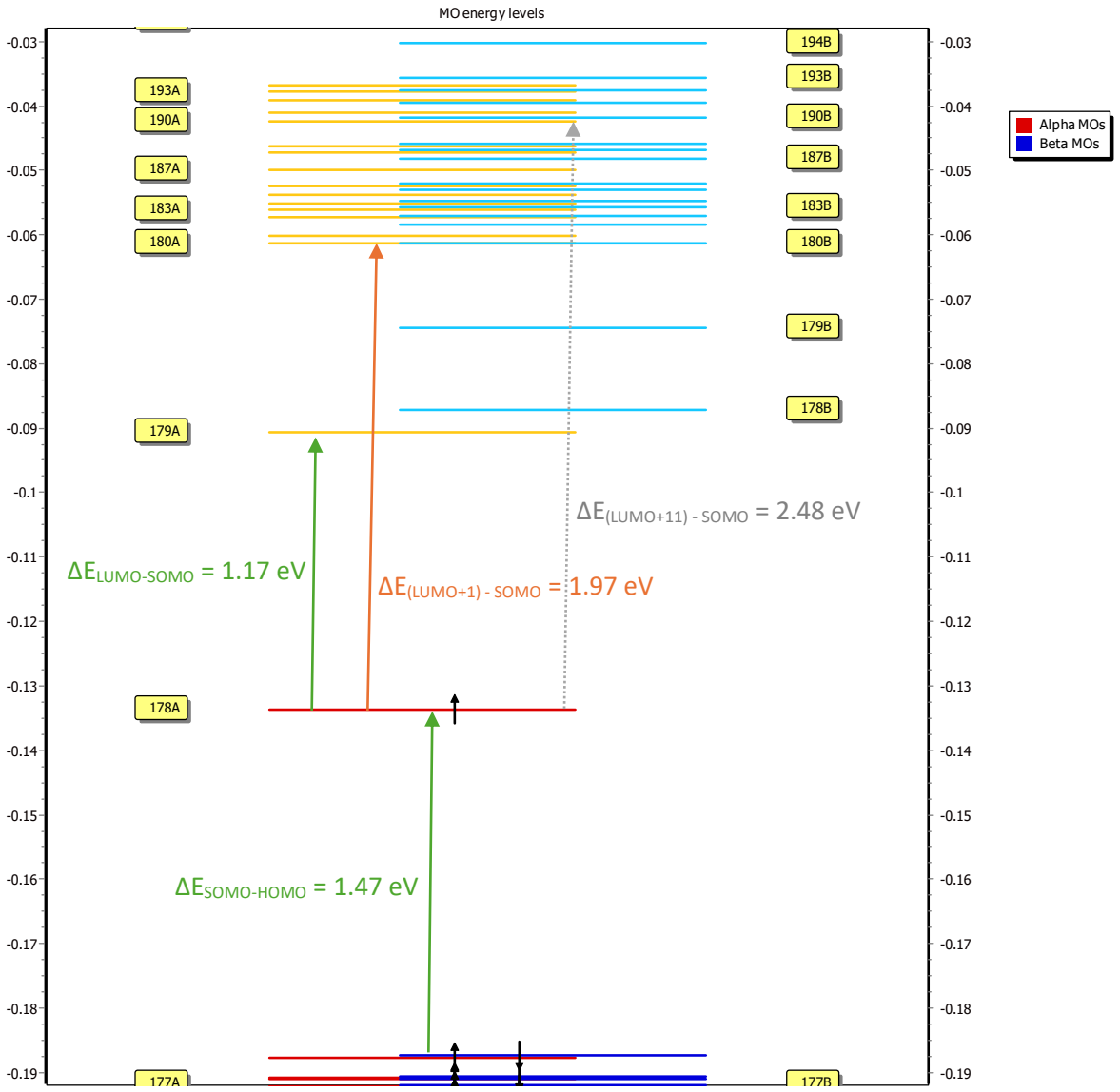

Fig. S4: DFT computed molecular orbital (MO) energy level diagram for complex **1**. Singly Occupied Molecular Orbital (SOMO) is π*-type where radical electron is delocalised mainly on the triazine moiety (see Fig. S4b). Green arrows show HOMO to SOMO and SOMO to LUMO energy separation in eV (1.47 and 1.17 eV, respectively). Orange color solid arrow shows SOMO to LUMO+1 electronic transition and dotted grey color arrow shows SOMO to LUMO+11 electronic transition. DFT calculation suggests all UV-Vis transitions in the range of 500 -750 nm are associated with singly occupied π*-Triazine radical molecular orbital (SOMO) to energetically closer empty π*-Triazine molecular orbital (LUMO) and uranium 5f-based MOs (between LUMO+1 and LUMO+11). See MOs diagram in Fig. S5 below.

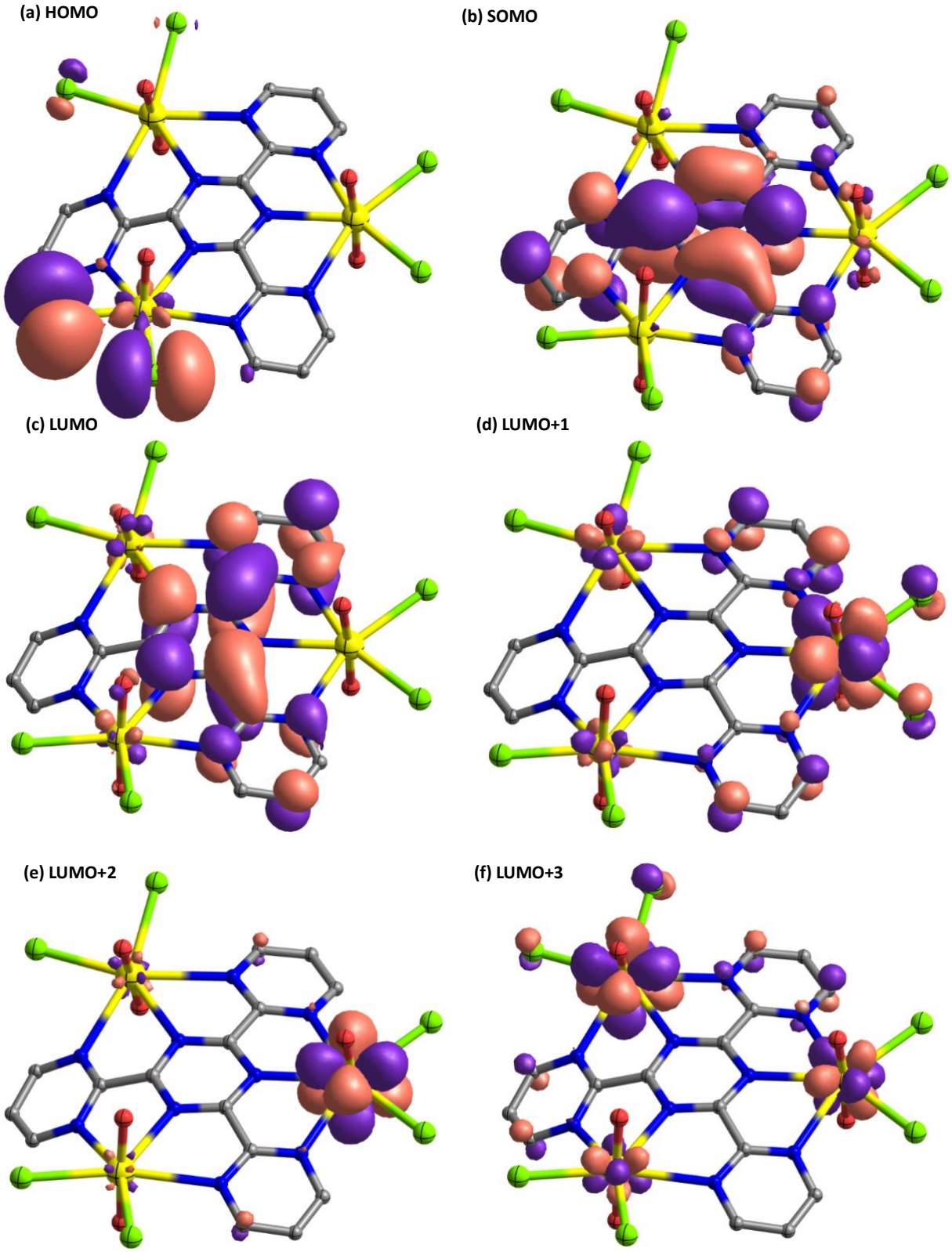

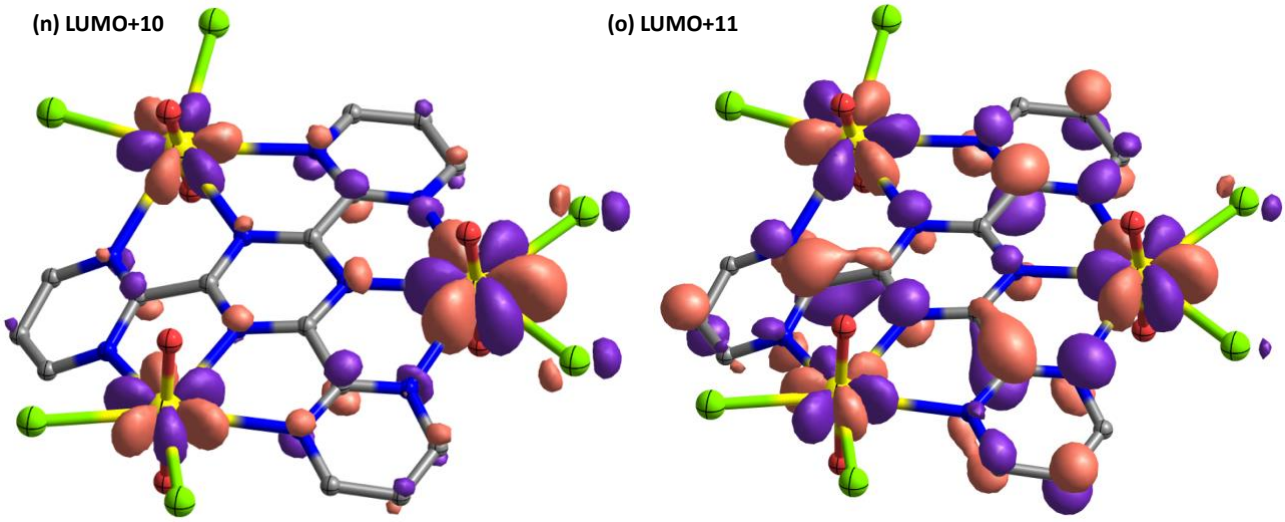

Fig. S5: DFT computed (a) HOMO, (b) SOMO, (c) LUMO, (d-o) LUMO+1 to LUMO+11 diagrams, respectively for **1**.

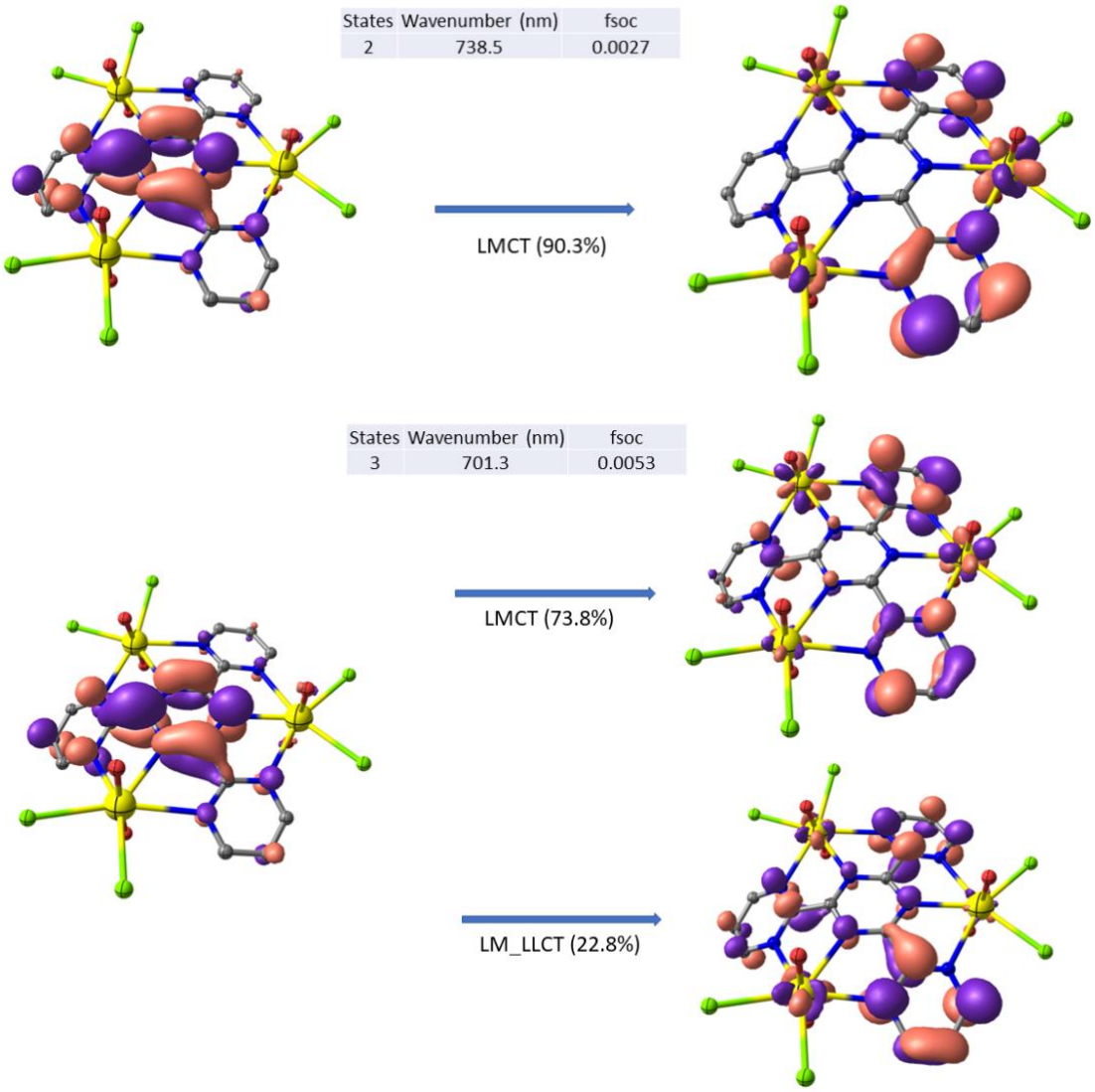
States Wavenumber (nm) fsoc
2 738.5 0.0027
LMCT (90.3%)
States Wavenumber (nm) fsoc
3 701.3 0.0053
LMCT (73.8%)
LM_LLCT (22.8%)

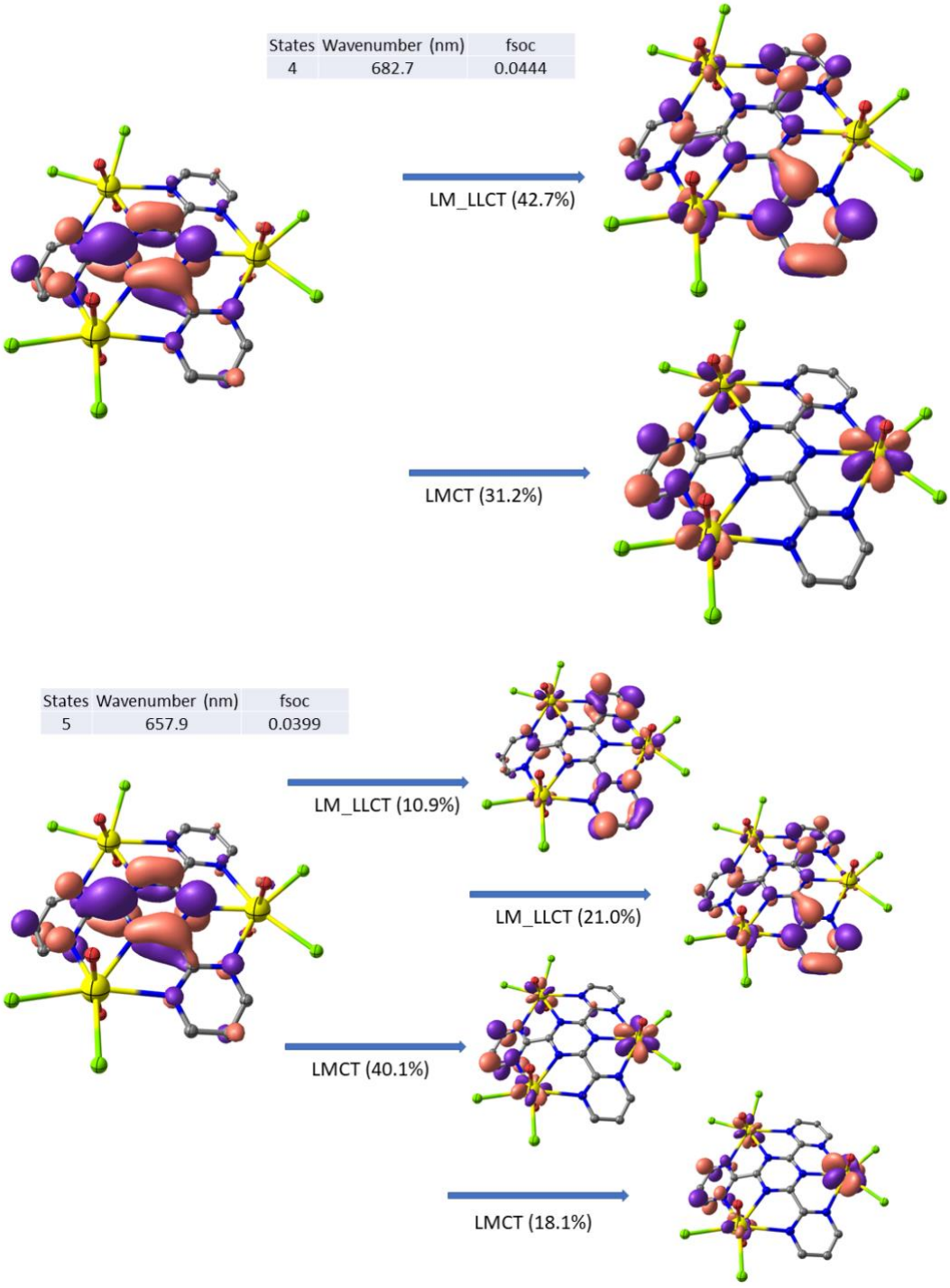
States Wavenumber (nm) fsoc
4 682.7 0.0444
LM_LLCT (42.7%)
LMCT (31.2%)
States Wavenumber (nm) fsoc
5 657.9 0.0399
LM_LLCT (10.9%)
LM_LLCT (21.0%)
LMCT (40.1%)
LMCT (18.1%)

States	Wavenumber (nm)	fsoc
6	648.9	0.0024

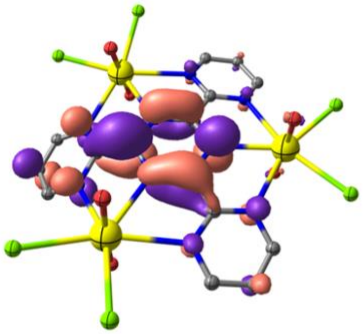

LMCT (23.5%)

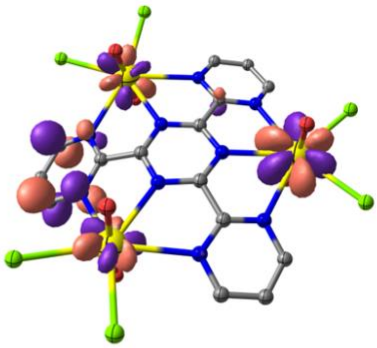

LMCT (73.1%)

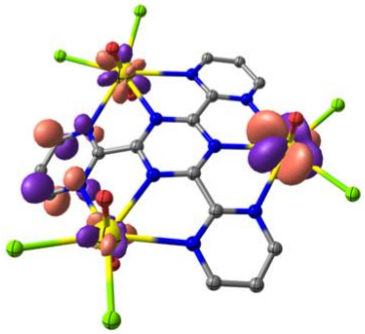

States	Wavenumber (nm)	fsoc
7	629.1	0.0092

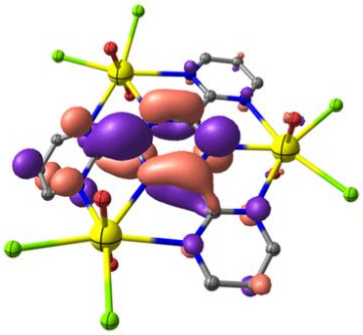

LMCT (70.8%)

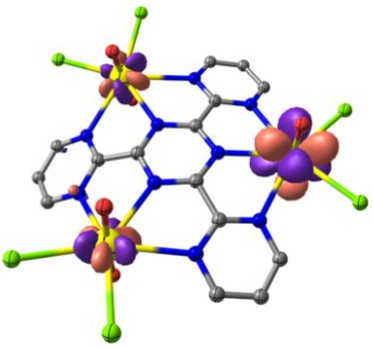

LMCT (24.3%)

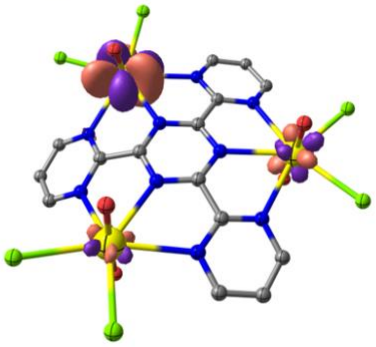

States	Wavenumber (nm)	fsoc
8	611.6	0.0340

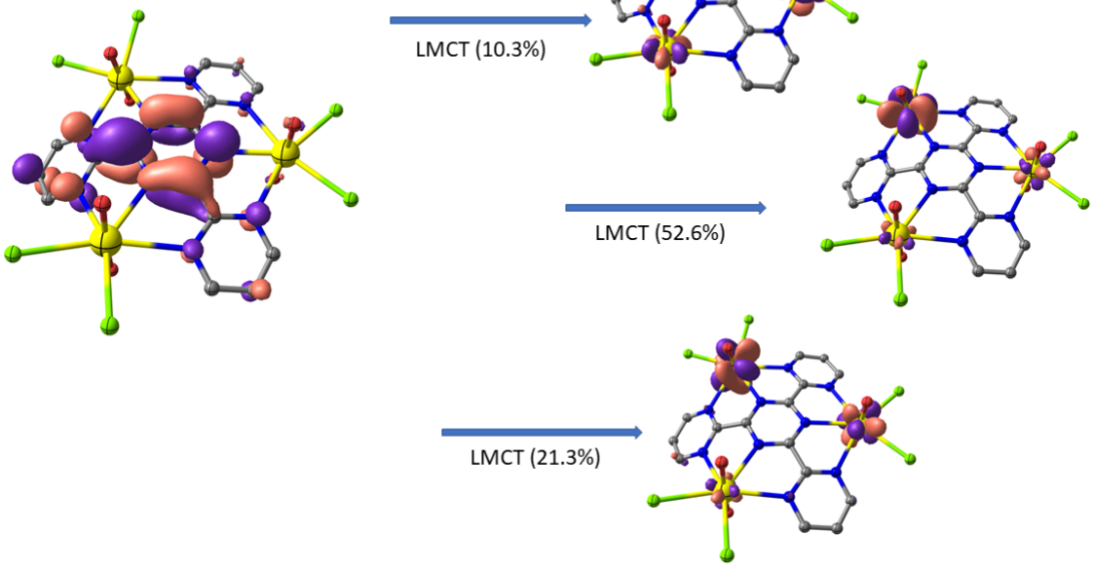

States	Wavenumber (nm)	fsoc
9	607.6	0.0183

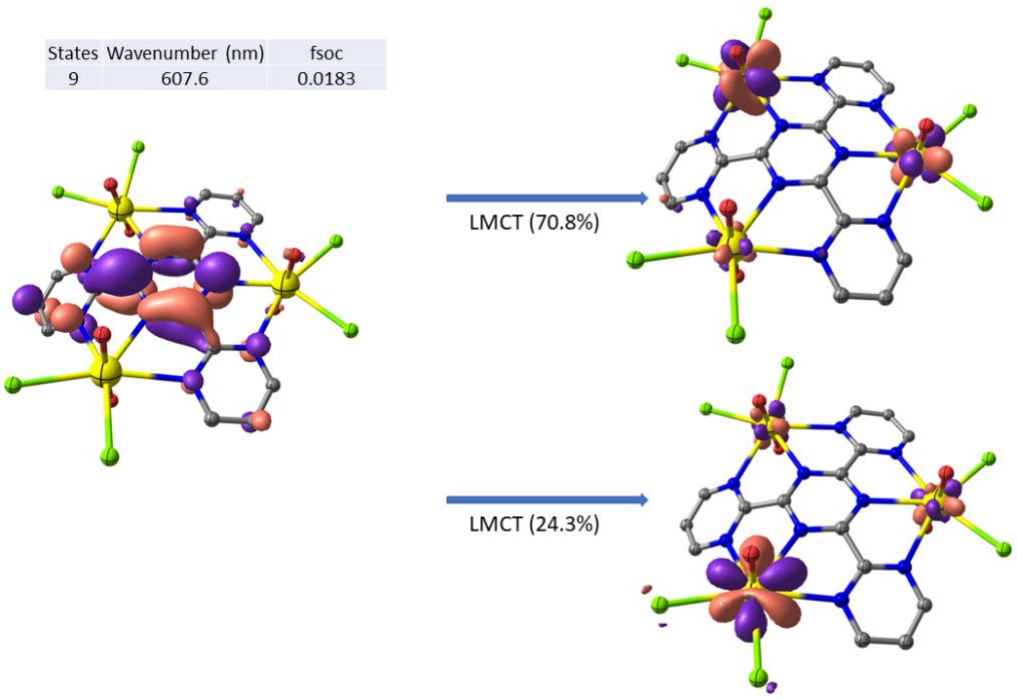

States	Wavenumber (nm)	fsoc
10	601.2	0.0181

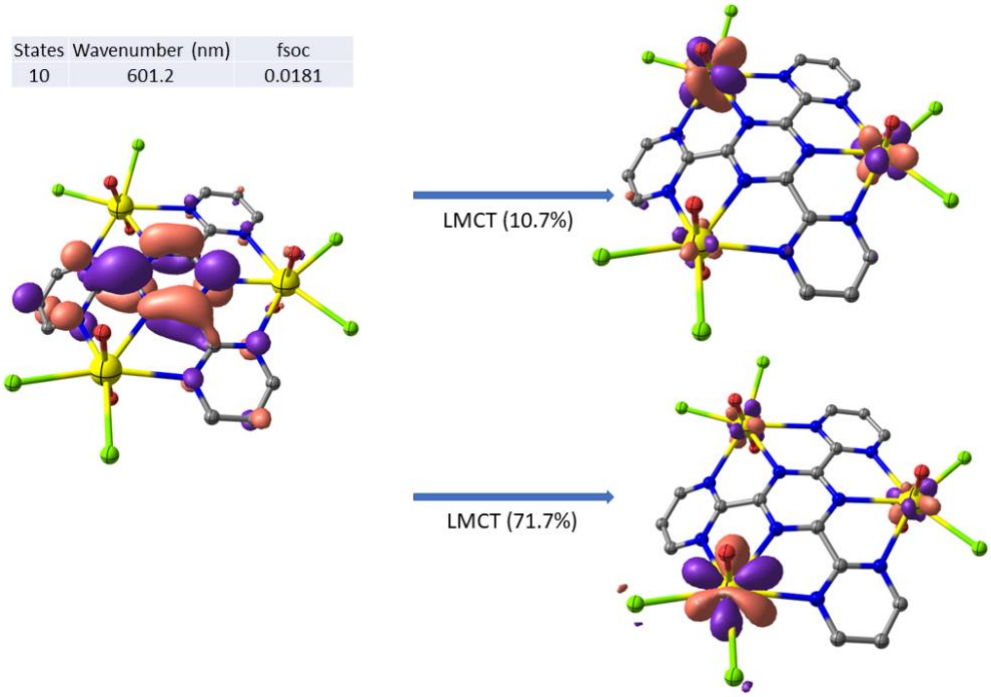

States	Wavenumber (nm)	fsoc
11	597.3	0.071

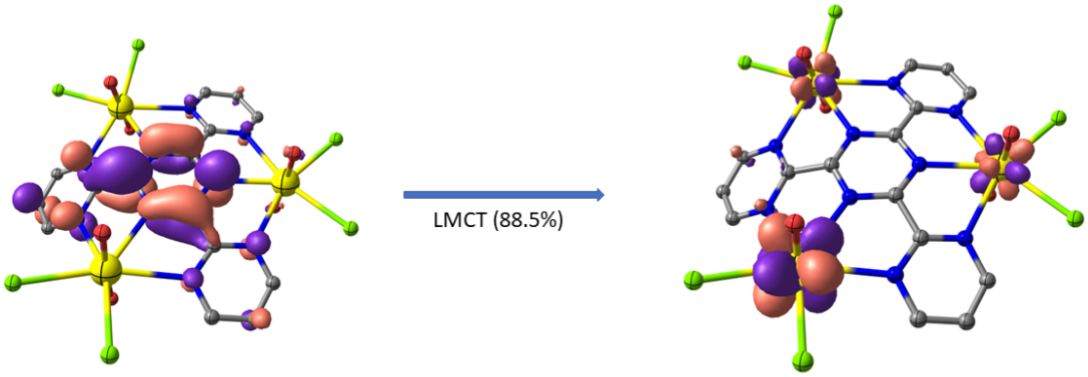

States	Wavenumber (nm)	fsoc
12	576.5	0.0117

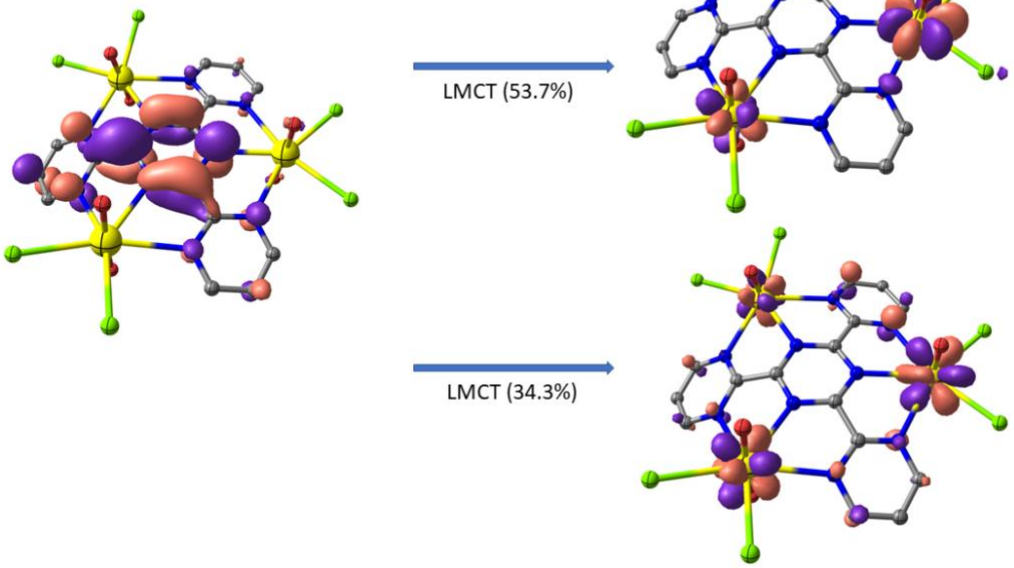

States	Wavenumber (nm)	fsoc
14	573.3	0.0057

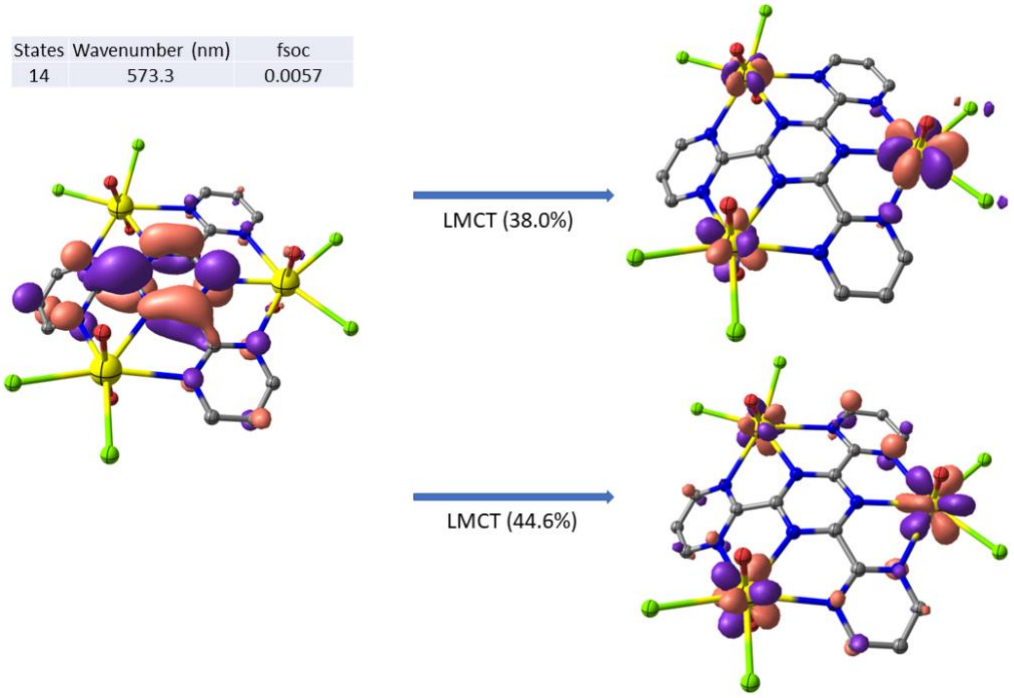

States	Wavenumber (nm)	fsoc
15	569.7	0.0021

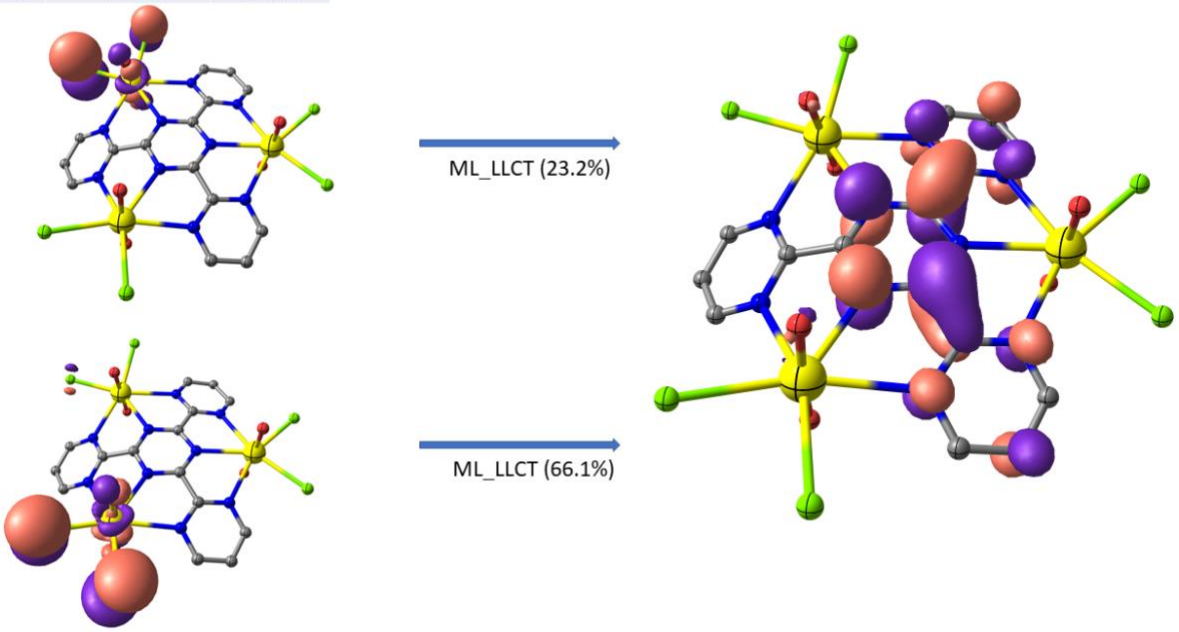

States	Wavenumber (nm)	fsoc
17	562.1	0.0059

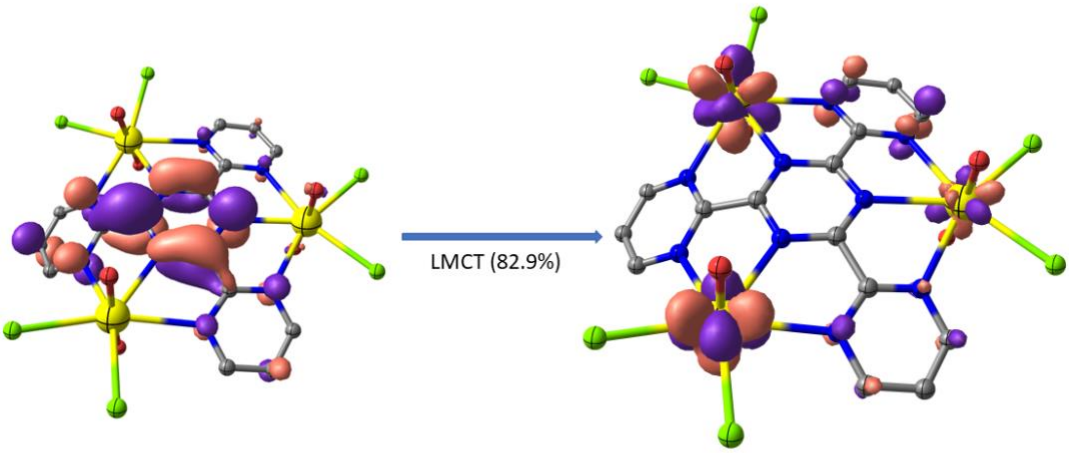

States	Wavenumber (nm)	fsoc
18	556.9	0.0016

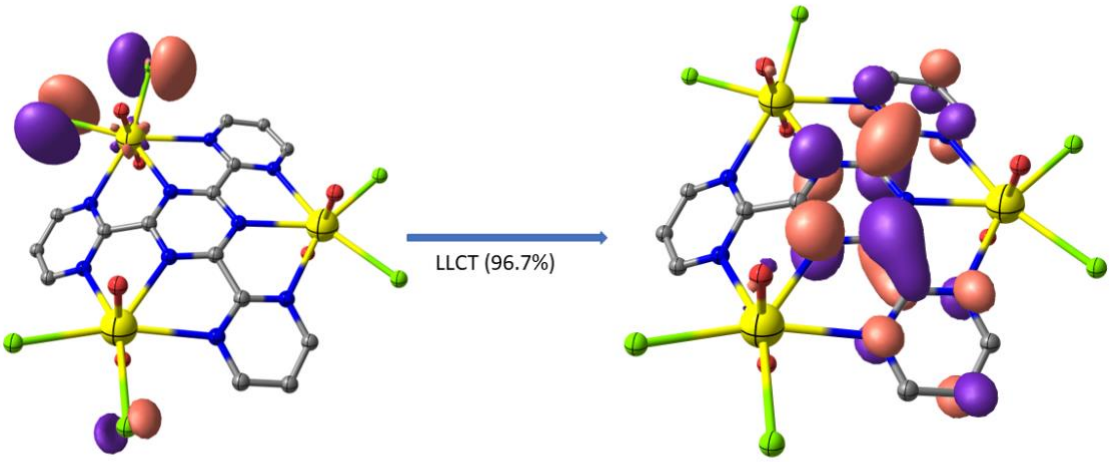

States	Wavenumber (nm)	fsoc
19	551.3	0.0077

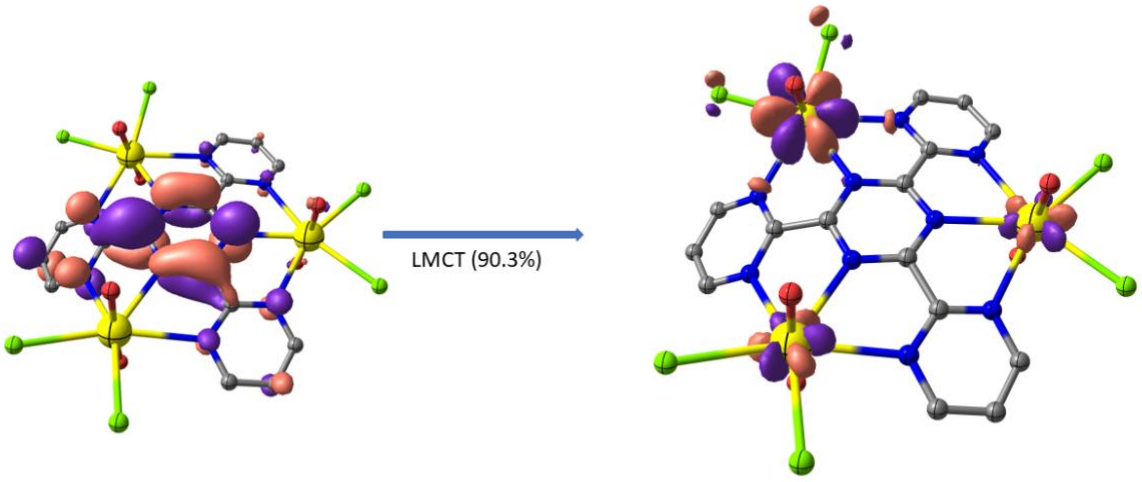

States	Wavenumber (nm)	fsoc
20	549.0	0.0020

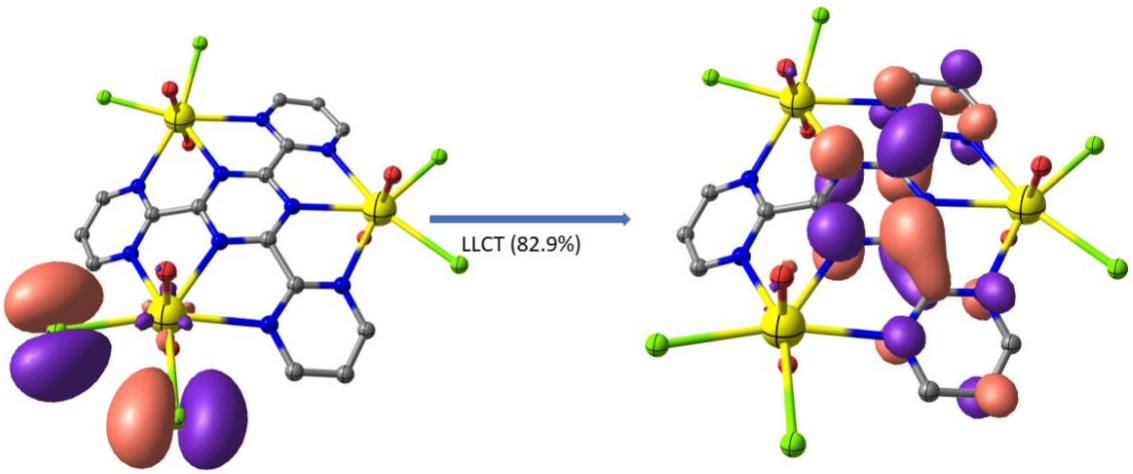

States	Wavenumber (nm)	fsoc
21	545.1	0.0014

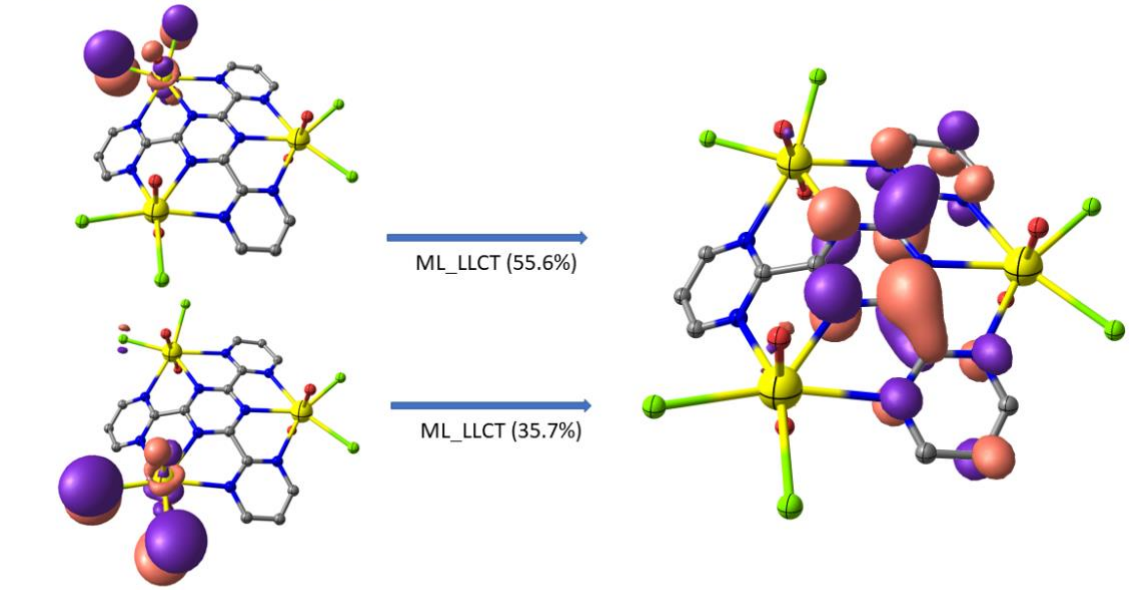

States	Wavenumber (nm)	fsoc
22	544.7	0.0026

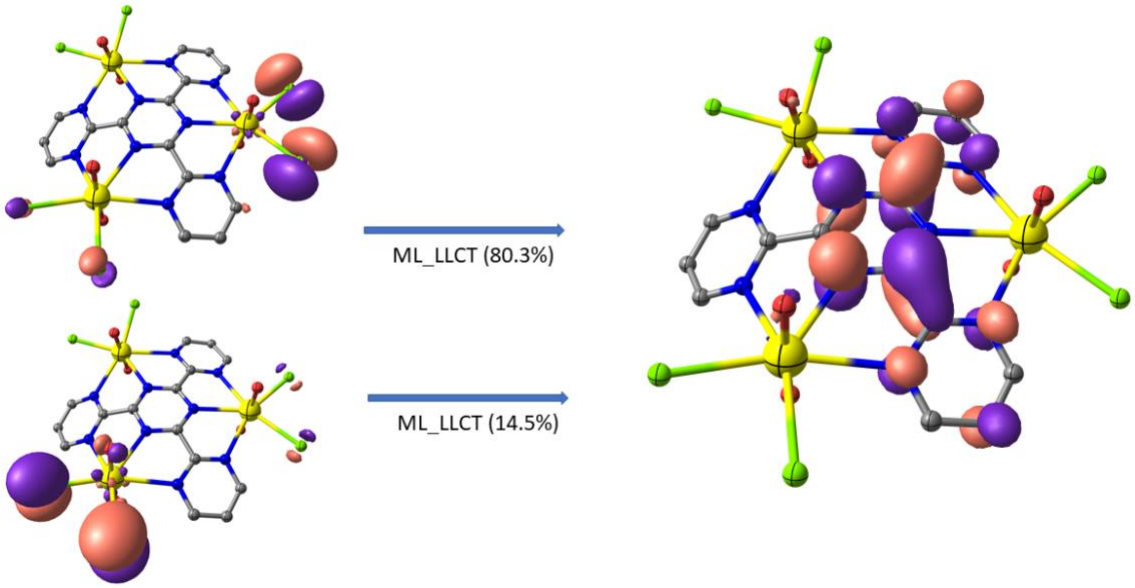

States	Wavenumber (nm)	fsoc
26	534.6	0.0021

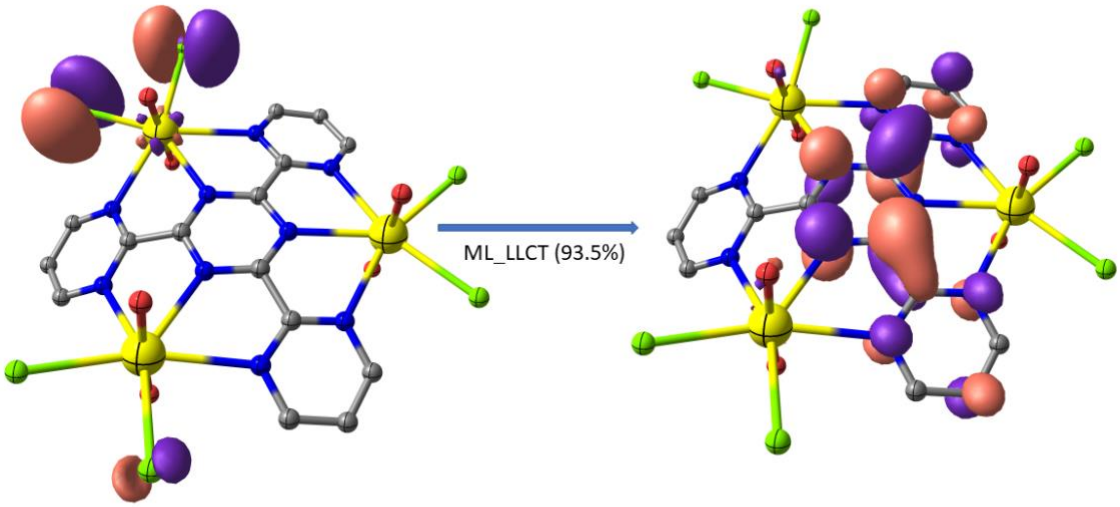

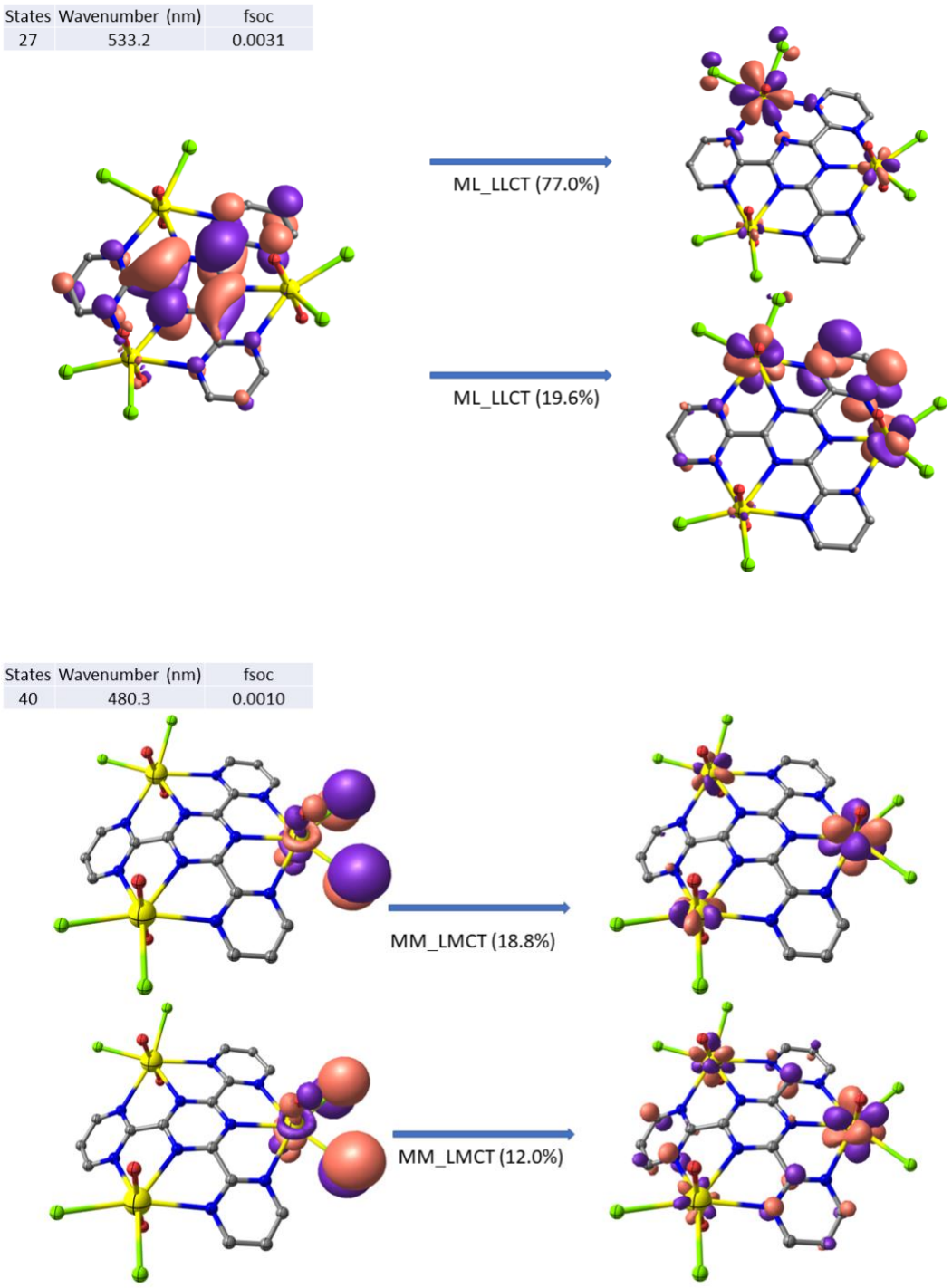

Fig. S6: Time-dependent DFT (TD-B3LYP) computed transition probabilities for complex **1** showing selected electronic transitions. For these states, any transitions with percentage contributions less than 10% are ignored.

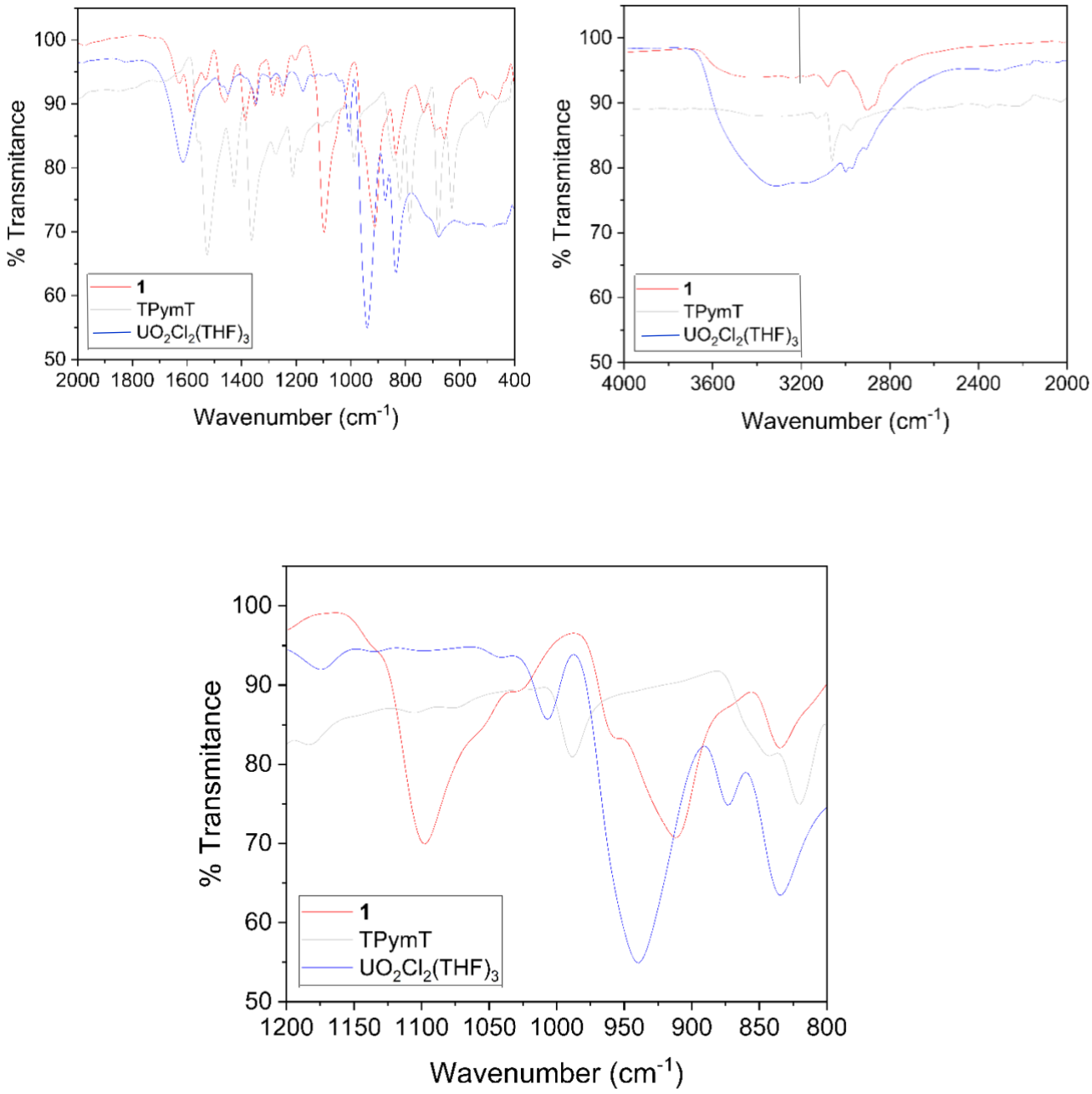

Fig. S7: Overlapped IR spectra for *Red*: **1**, *Light grey*: TPymT and *Blue*: $UO_2Cl_2(THF)_3$.

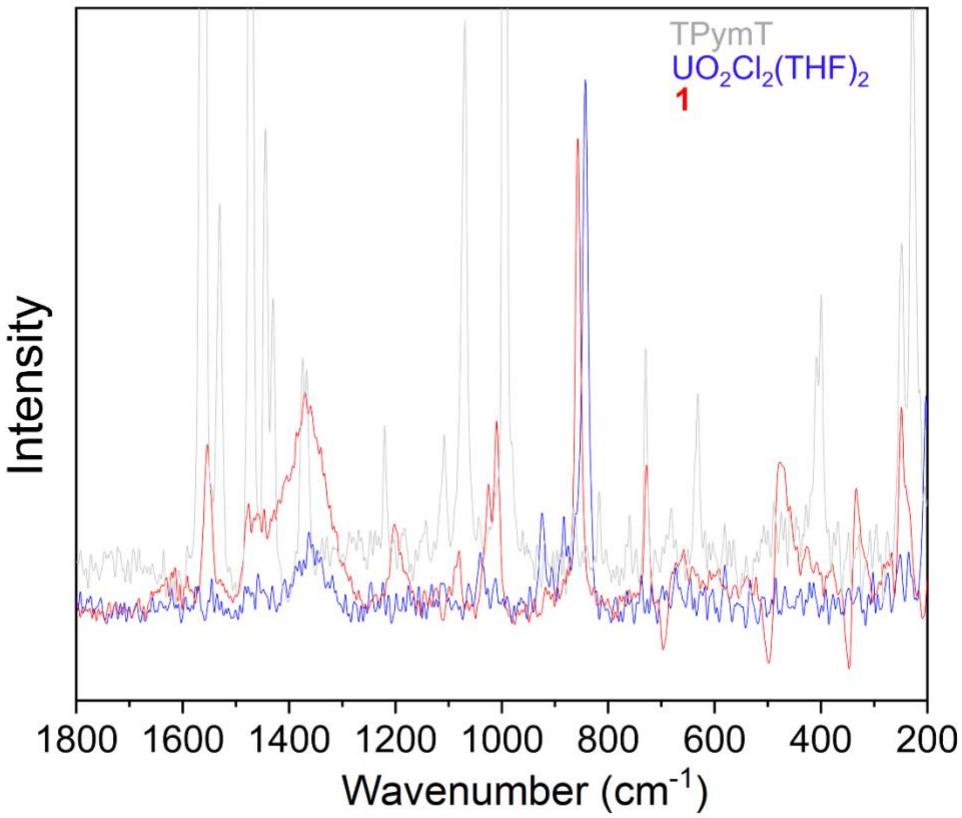

Fig. S8: Overlapped Raman spectra for *Red*: **1**, *Light grey*: TPymT and *Blue*: $UO_2Cl_2(THF)_3$.

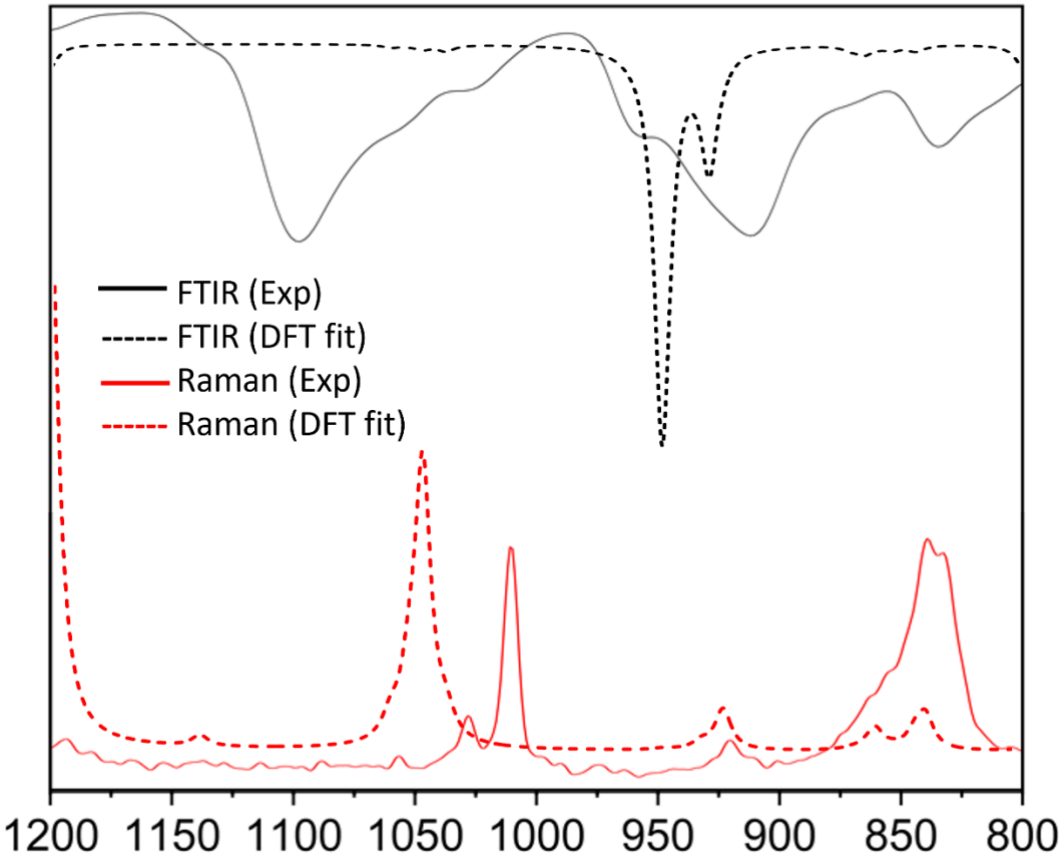

Fig. S9: Experimental FTIR, Raman and DFT computed spectra for **1**. Note: calculations were conducted on the core structure of **1**, $[(UO_2Cl_2)_3(TPymT)]^{\bullet-}$, and thus the strong absorption at 1100 cm^{-1} corresponding to $[K\{18\text{-c-}6\}]^+$, is not reproduced from the calculation.

References.

1. (a) M. P. Wilkerson, C. J. Burns, R. T. Paine and B. L. Scott, *Inorg. Chem.*, 1999, **38**, 4156-4158; (b) D. A. Safin, N. A. Tumanov, A. A. Leitch, J. L. Brusso, Y. Filinchuk and M. Murugesu, *CrystEngComm*, 2015, **17**, 2190-2195.
2. G. M. Sheldrick, *Acta Crystallogr., Sect. A: Found. Adv.*, 2015, **71**, 3.
3. O. V. Dolomanov, L. J. Bourhis, R. J. Gildea, J. A. K. Howard and H. Puschmann, *J. Appl. Crystallogr.*, 2009, **42**, 339.
4. C. F. Macrae, I. Sovago, S. J. Cottrell, P. T. A. Galek, P. McCabe, E. Pidcock, M. Platings, G. P. Shields, J. S. Stevens, M. Towler and P. A. Wood, *J. Appl. Crystallogr.*, 2020, **53**, 226-235.
5. G. R. Hanson, K. E. Gates, C. J. Noble, M. Griffin, A. Mitchell and S. Benson, S. *J. Inorg. Biochem.*, 2004, **98**, 903.
6. (a) T. Lu and F. Chen, *J. Comput. Chem.*, 2012, **33**, 580-592; (b) H. L. Schmider and A. D. Becke, *J. Mol. Struct. THEOCHEM.*, 2000, **527**, 51-61.
7. (a) L. K. Harper, A. L. Shoaf and C. A. Bayse, *ChemPhysChem*, 2015, **16**, 3886-3892; (b) I. Mayer, *J. Comput. Chem.*, 2007, **28**, 204-221; (c) K. B. Wiberg, *Tetrahedron*, 1968, **24**, 1083-1096.
8. M. J. Frisch, G. W. Trucks, H. B. Schlegel, G. E. Scuseria, M. A. Robb, J. R. Cheeseman, G. Scalmani, V. Barone, G. A. Petersson, H. Nakatsuji, X. Li, M. Caricato, A. V. Marenich, J. Bloino, B. G. Janesko, R. Gomperts, B. Mennucci, H. P. Hratchian, J. V. Ortiz, A. F. Izmaylov, J. L. Sonnenberg, Williams, F. Ding, F. Lipparini, F. Egidi, J. Goings, B. Peng, A. Petrone, T. Henderson, D. Ranasinghe, V. G. Zakrzewski, J. Gao, N. Rega, G. Zheng, W. Liang, M. Hada, M. Ehara, K. Toyota, R. Fukuda, J. Hasegawa, M. Ishida, T. Nakajima, Y. Honda, O. Kitao, H. Nakai, T. Vreven, K. Throssell, J. A. Montgomery Jr., J. E. Peralta, F. Ogliaro, M. J. Bearpark, J. J. Heyd, E. N. Brothers, K. N. Kudin, V. N. Staroverov, T. A. Keith, R. Kobayashi, J. Normand, K. Raghavachari, A. P. Rendell, J. C. Burant, S. S. Iyengar, J. Tomasi, M. Cossi, J. M. Millam, M. Klene, C. Adamo, R. Cammi, J. W. Ochterski, R. L. Martin, K. Morokuma, O. Farkas, J. B. Foresman and D. J. Fox, Gaussian16, 2016.
9. (a) A. D. Becke, *J. Chem. Phys.*, 1993, **98**, 5648; (b) C. Lee, W. Yang and R. G. Parr, *Phys. Rev. B: Condens. Matter Mater. Phys.*, 1988, **37**, 785; (c) P. J. Stephens, F. J. Devlin, C. F. Chabalowski and M. J. Frisch, *J. Phys. Chem.*, 1994, **98**, 11623-11627.
10. W. C. Ermler, R. B. Ross and P. A. Christiansen, *Int. J. Quantum Chem*, 1991, **40**, 829-846.
11. A. Schafer, H. Horn and R. Ahlrichs, *J. Chem. Phys.*, 1992, **97**, 2571-2577.
12. (a) M. K. Singh, A. Etcheverry-Berríos, J. Vallejo, S. Sanz, J. Martínez-Lillo, G. S. Nichol, P. J. Lusby and E. K. Brechin, *Dalton Trans.*, 2022, **51**, 8377-8381; (b) E. K. Brechin, D. J. Cutler, M. Coletta, M. Singh, A. B. Tsanai, L. J. McCormick McPherson, S. Coles and J. Schnack, *Dalton Trans.*, 2022, **51**, 8945-8948; (c) E. Agapaki, M. K. Singh, A. B. Canaj, G. S. Nichol, J. Schnack and E. K. Brechin, *Chem. Commun.*, 2022, **58**, 9088-9091; (d) P. A. Tsami, T. G. Tziotzi, A. B. Canaj, M. K. Singh, S. J. Dalgarno, E. K. Brechin and C. J. Milios, *Dalton Trans.*, 2022, **51**, 15128-15132; (e) M. Coletta, T. G. Tziotzi, M. Gray, G. S. Nichol, M. K. Singh, C. J. Milios and E. K. Brechin, *Chem. Commun.*, 2021, **57**, 4122-4125; (f) D. J. Cutler, M. K. Singh, G. S. Nichol, M. Evangelisti, J. Schnack, L. Cronin and E. K. Brechin, *Chem. Commun.*, 2021, **57**, 8925-8928; (g) M. K. Singh, *Dalton Trans.*, 2020, **49**, 4539–4548; (h) M. Coletta, S. Sanz, D. J. Cutler, S. J. Teat, K. J. Gagnon, M. K. Singh, E. K. Brechin and S. J. Dalgarno, *Dalton Trans.*, 2020, **49**, 14790-14797; (i) Y. Peng, M. K. Singh, V. Mereacre, C. E. Anson, G. Rajaraman and A. K. Powell, *Chem. Sci.*, 2019, **10**, 5528-5538; (j) M. K. Singh and G. Rajaraman, *Inorg. Chem.*, 2019, **58**, 3175-3188; (k) M. K. Singh, T. Rajeshkumar, R. Kumar, S. K. Singh and G. Rajaraman, *Inorg. Chem.*, 2018, **57**, 1846-1858; (l) S. Ghosh, S. Mandal, M.

K. Singh, C.-M. Liu, G. Rajaraman and S. Mohanta, *Dalton Trans.*, 2018, **47**, 11455-11469; (m) M. K. Singh, N. Yadav and G. Rajaraman, *Chem Commun (Camb)*, 2015, **51**, 17732-17735; (n) M. K. Singh and G. Rajaraman, *Chem. Eur. J.*, 2015, **21**, 980-983; (o) A. Upadhyay, J. Rajpurohit, M. Kumar Singh, R. Dubey, A. K. Srivastava, A. Kumar, G. Rajaraman and M. Shanmugam, *Chem. Eur. J.*, 2014, **20**, 6061-6070; (p) S. Hazra, S. Bhattacharya, M. K. Singh, L. Carrella, E. Rentschler, T. Weyhermueller, G. Rajaraman and S. Mohanta, *Inorg. Chem.*, 2013, **52**, 12881-12892.

13. F. Neese, *WIREs Comput. Mol. Sci.*, 2022, **12**, e1606.
14. (a) F. Weigend and R. Ahlrichs, *Phys. Chem. Chem. Phys.*, 2005, **7**, 3297; (b) F. Weigend, *Phys. Chem. Chem. Phys.*, 2006, **8**, 1057; (c) F. Weigend, F. Furche and R. Ahlrichs, *J. Chem. Phys.*, 2003, **119**, 12753-12762.